

2005

# Eye movement responses to angular and linear motion in wild type and het mice

Patricia Milagros Chang  
*San Jose State University*

Follow this and additional works at: [https://scholarworks.sjsu.edu/etd\\_theses](https://scholarworks.sjsu.edu/etd_theses)

---

## Recommended Citation

Chang, Patricia Milagros, "Eye movement responses to angular and linear motion in wild type and het mice" (2005). *Master's Theses*. 2862.

DOI: <https://doi.org/10.31979/etd.geu2-ucjp>

[https://scholarworks.sjsu.edu/etd\\_theses/2862](https://scholarworks.sjsu.edu/etd_theses/2862)

This Thesis is brought to you for free and open access by the Master's Theses and Graduate Research at SJSU ScholarWorks. It has been accepted for inclusion in Master's Theses by an authorized administrator of SJSU ScholarWorks. For more information, please contact [scholarworks@sjsu.edu](mailto:scholarworks@sjsu.edu).

# NOTE TO USERS

This reproduction is the best copy available.

**UMI**<sup>®</sup>



EYE MOVEMENT RESPONSES TO ANGULAR AND LINEAR MOTION IN WILD  
TYPE AND *HET* MICE

A Thesis

Presented to

The Faculty of the Department of Biological Sciences

San Jose State University

In Partially Fulfillment

of the Requirements for the Degree

Master of Science

by

Patricia Milagros Chang

December 2005

UMI Number: 1432480

Copyright 2005 by  
Chang, Patricia Milagros

All rights reserved.

### INFORMATION TO USERS

The quality of this reproduction is dependent upon the quality of the copy submitted. Broken or indistinct print, colored or poor quality illustrations and photographs, print bleed-through, substandard margins, and improper alignment can adversely affect reproduction.

In the unlikely event that the author did not send a complete manuscript and there are missing pages, these will be noted. Also, if unauthorized copyright material had to be removed, a note will indicate the deletion.

**UMI**<sup>®</sup>

---

UMI Microform 1432480

Copyright 2006 by ProQuest Information and Learning Company.

All rights reserved. This microform edition is protected against  
unauthorized copying under Title 17, United States Code.

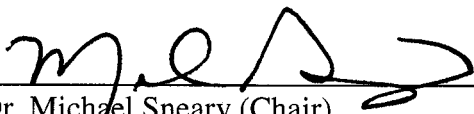
ProQuest Information and Learning Company  
300 North Zeeb Road  
P.O. Box 1346  
Ann Arbor, MI 48106-1346

© 2005

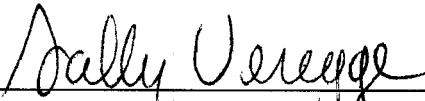
Patricia Milagros Chang

ALL RIGHTS RESERVED


APPROVED FOR THE DEPARTMENT OF BIOLOGICAL SCIENCES

  
\_\_\_\_\_  
Dr. Michael Sneary (Chair)

  
\_\_\_\_\_  
Dr. Geoffrey Bush (Scientist, NASA Ames Research Center)

  
\_\_\_\_\_  
Dr. Sally Veregge (Department Chair)

APPROVED FOR SAN JOSE STATE UNIVERSITY

  
\_\_\_\_\_

## ABSTRACT

### EYE MOVEMENT RESPONSES TO ANGULAR AND LINEAR MOTION IN WILD TYPE AND *HET* MICE

By Patricia Milagros Chang

Astronauts exposed to altered gravity environments frequently develop motion sickness in orbit and temporary balance problems upon return to Earth. The central nervous system has the ability to make new connections or use existing connections in different ways to respond to such a changing environment. The present study compares the compensatory oculomotor reflex to head movement in a wild type and a genetically altered mouse known as the *Head Tilt* mouse (*het*) that lacks normal gravito-inertial sensors. Experiments of this type may help us understand how the nervous system responds to novel environments, such as the condition of microgravity in space. The results of this study may also serve to improve therapies for patients with vestibular disorders.



## ACKNOWLEDGEMENTS

This study was undertaken in the Vestibular Research Facility, the Biological Visualization, Imaging, and Simulation (BioVIS) laboratory of Dr. Richard Boyle at NASA Ames Research Center. I would like to thank Dr. Richard Boyle for introducing me to wonderful scientists, Dr. Michael Sneary and Dr. Geoffrey Bush. I also want to thank for all the sophisticated equipments provided by Dr. Richard Boyle and Dr. Geoffrey Bush and the lovely people of this team like Joseph Varelas (SEM imaging), Reza Ehsanian, Stan Hardy, Rei Cheng, and Xander Twonbly. All of them became my mentors as time went by and their encouragement helped me to decide my professional goals. They kept me on track and gave me valuable advices to pursue my dreams. I would like to thank Dr. Larry Hoffman from the University of Los Angeles for providing us the animal model. Also, I would like to thank Stephen Voels, John Waltkins, James Connolly, Gabino Chu, and Ricardo Wu for helping us in the IGOR program. I am grateful to the members of my committee, especially Dr. Michael Sneary, Dr. Geoffrey Bush, and Dr. Sally Veregge for their advice and criticism in this thesis. I would like to thank to all the members of Animal Care Facility at NASA and Larry Young from San Jose State University. Also, I would like to thank the Education Associate (EA) program specially Carol Roland and Teresa Scherbing for the wonderful opportunity at NASA. Finally, I would like to thank my parents (Pedro Chang & Dolores de Chang), my brother (Pedro Chang) and his wife (Liz Chang-Morales), my cousins (Julito Alcantara & Gabino Chu), all the family, and friends (e.g., Max Sanchez, Elisa Lau, Ines Giraldo, Ricardo Wu) for all their support, love, encouragement, and dedication to be who I am now.

## TABLE OF CONTENTS

	<u>Page</u>
INTRODUCTION	1
I. Peripheral Vestibular System	1
A. Sensory Hair Cells and Vestibular Nerve Fibers	1
B. Semicircular Canals	2
C. Otolith Organs	3
II. Vestibulo Ocular Reflex	4
III. <i>Het</i> Mice	6
IV. Purpose	8
MATERIALS AND METHODS	11
I. Mice	11
II. Surgery	12
III. Coil Fabrication and Calibration	13
IV. Equipment	14
V. Stimulus Paradigms	14
VI. Data Analysis	15
VII. Histology	16
VIII. Scanning Electron Microscopy (SEM)	17
RESULTS	18
I. Microscopy of the Otoconial Mass in the <i>Het</i> Mouse	18

II. Vestibulo-ocular Reflex	18
A. General Features of Vertical Axis Horizontal VOR	18
B. Frequency Dynamics of Control Group and <i>Het</i> Mice	19
C. Gain and Phase Results of both Control Group and <i>Het</i> Mice	
DISCUSSION	21
BIBLIOGRAPHY	26
APPENDIX: FIGURES	
Figure 1. Vestibulo-ocular Reflex (VOR) Bio-circuit	A-1
Figure 2. Scleral Search Coil	A-2
Figure 3. Animal Restraint Apparatus	A-3
Figure 4. Multi-axis Centrifuge; Vestibular Research Facility	A-4
Figure 5. Abnormal Structures of the Otoconia Formation SEM	A-5
Figure 6. Amplitude 2 at 0.05Hz of Control Group	A-6
Figure 7. Amplitude 2 at 0.1Hz of Control Group	A-7
Figure 8. Amplitude 2 at 0.25Hz of Control Group	A-7
Figure 9. Amplitude 2 at 0.5Hz of Control Group	A-8
Figure 10. Amplitude 2 at 1Hz of Control Group	A-8
Figure 11. Amplitude 2 at 2Hz of Control Group	A-9
Figure 12. Amplitude 3 at 0.05Hz of Control Group	A-10

Figure 13. Amplitude 3 at 0.1Hz of Control Group	A-11
Figure 14. Amplitude 3 at 0.25Hz of Control Group	A-12
Figure 15. Amplitude 3 at 0.5Hz of Control Group	A-13
Figure 16. Amplitude 3 at 1Hz of Control Group	A-14
Figure 17. Amplitude 2 at 0.05Hz of <i>Het</i> Mice	A-15
Figure 18. Amplitude 2 at 0.1Hz of <i>Het</i> Mice	A-15
Figure 19. Amplitude 2 at 0.25Hz of <i>Het</i> Mice	A-16
Figure 20. Amplitude 2 at 0.5Hz of <i>Het</i> Mice	A-16
Figure 21. Amplitude 2 at 1Hz of <i>Het</i> Mice	A-17
Figure 22. Amplitude 2 at 2Hz of <i>Het</i> Mice	A-17
Figure 23. Amplitude 3 at 0.05Hz of <i>Het</i> Mice	A-18
Figure 24. Amplitude 3 at 0.1Hz of <i>Het</i> Mice	A-18
Figure 25. Amplitude 3 at 0.25Hz of <i>Het</i> Mice	A-19
Figure 26. Amplitude 3 at 0.5Hz of <i>Het</i> Mice	A-19
Figure 27. Amplitude 3 at 1Hz of <i>Het</i> Mice	A-20
Figure 28. Bode Diagram of Gain and Phase at Amplitude 2 (50°/s)	A-21
Figure 29. Bode Diagram of Gain and Phase at Amplitude 3 (100°/s)	A-22
Figure 30. Function of the Vestibular System	A-23

## INTRODUCTION

### *I. Peripheral Vestibular System*

The function of the vestibular system in vertebrates is to maintain balance, stabilize vision, and control movement (2, 27). The system includes five peripheral sensory organs associated with each ear: three semicircular canals (superior, posterior, and lateral or horizontal) for angular accelerations of the head and two otolith organs for translational and gravito-inertial accelerations (sacculle and utricle).

#### *A. Sensory Hair Cells and Vestibular Nerve Fibers*

The hair cells are the sensory receptors of the vestibular labyrinth and are responsible for mechano-electrical transduction that sends electrical signals to the brain for analysis via the afferent nerve fibers of the 8<sup>th</sup> cranial nerve. There are three kinds of afferent nerve fibers, each with a different termination; calyx fibers, bouton fibers, and dimorphic fibers. Calyx fibers have terminations that completely surround the basolateral surface of the target hair cell(s). These fibers innervate a region of the epithelium called the striola. Bouton fibers have terminations that make smaller, distinct contacts with the target hair cell(s). These fibers may be found throughout the epithelium. Dimorphic fibers provide a mixed innervation, including calyx and bouton endings. Dimorphic units also supply the entire sensory epithelium (13, 9). Efferent nerve fibers, whose cell bodies are in the brain, serve to modulate sensory input. Efferent nerve fibers may contact hair cells and/or afferent nerve fibers.

The apical surface is in contact with a fluid filled (endolymphatic) space that is high in potassium concentration. Tight junctions at the apical surface of the hair cells

separate apical and basolateral fluid spaces. The hair bundle, composed of stereocilia (microvilli in reptiles, birds, and mammals) and a single kinocilium (true cilium), projects into the endolymphatic space. Deflection of the hair bundle toward the kinocilium opens cation channels and allows the entrance of  $K^+$  from the endolymph into the hair cells. The hair cell is then depolarized, opening voltage-gated  $Ca^{2+}$  channels in the basolateral membrane. The subsequent influx of  $Ca^{2+}$  triggers the release of neurotransmitter, which in turn causes an increase in the frequency of action potentials in the vestibular afferents (10, 16, 20, 27).

### *B. Semicircular Canals*

Each semicircular canal is essentially donut-shaped with a dilated end called an ampulla where the sensory epithelium is located. The three (lateral, superior, and posterior) canals are laid out in nearly orthogonal planes. Each canal is nearly co-planar with the corresponding canal on the other side. The canal consists of a circular tube filled with viscous endolymphatic fluid. The ampullar space is blocked by a small triangular shaped mass of gelatinous material called the cupula. This structure sits on a bulge in the wall called the crista that is covered with hair cells. When the head is rotated, the fluid lags behind because of its inertia and pushes against the cupula. The bundles in contact with the cupula are deflected and a transduction cascade is generated leading to action potentials in the afferent nerve fiber (10, 16). An individual canal is maximally sensitive to rotation of the head in its primary plane. Thus, the three canals, whose input is combined in the central nervous system, provide the organism with the ability to sense head rotations in any direction in three-dimensional space.

In general, the lateral (horizontal) semicircular canals have a plane that is elevated 10-30 degrees from the transverse while the vertically oriented superior (anterior) and posterior canals are in planes approximately 90 degrees from each other and both are laterally askew from the sagittal and the coronal planes, respectively. The canals function as organized pairs (i.e., the canal from the same plane on the opposite side of the head). For example, the superior semicircular canal on one side lies in the same plane as the posterior canal on the other side, and both detect angular acceleration in the same plane. Therefore, any head rotation can be encoded by the combined activity from multiple semicircular canals (10).

### *C. Otolith Organs*

The otolith organs include the utricle and the saccule. The sensory epithelium, called the macula, responds to linear accelerations such as those produced by translational motion or re-orientations of the head with respect to gravity. The utricular maculae sense movement mainly in the horizontal plane (e.g., left-right movement, forward-backward movement, and any combination thereof) (7, 10, 27). The saccular maculae sense motions in the sagittal plane (e.g., up-down movement). The sensory epithelia of the otolith organs are organized as essentially flat structures (horizontal for the utricle, and vertical for the saccule). In the epithelium, the hair cells are neighbored by supporting cells that not only support the hair cells metabolically but also secrete the extracellular matrix proteins that condense to form the overlying gelatinous otoconial membrane (10, 27). In mammals, this membrane contains two layers; the gelatinous layer and the otoconial layer (21). The gelatinous layer contains both amorphous and

fibrotic material. In the region of the macular striola, this structure is perforated by holes through which stereociliary bundles project. In other regions this structure is solid. The otoconial layer is composed of calcium carbonate crystals (otoconia) that are embedded in the gelatinous layer. Beneath the otoconial membrane are the hair cells whose bundles extend upward and are attached to the membrane via the bulb of the kinocilium. The otoconial layer has a higher specific gravity than endolymph. Motion of the head due to linear translation or reorientation of the head with respect to gravity results in the relative movement of the otoconial mass due to its inertia, and therefore stimulates the macular hair cells by deflecting the hair bundle.

## ***II. Vestibulo Ocular Reflex***

The vestibulo ocular reflex (VOR) maintains the stability of the image of the visual field in response to motion of the head; hence, the oculomotor system interacts with the vestibular system to produce compensatory eye movements (8,15). The VOR counter-rotates the eyes during head or whole body movement in order to maintain visual fixation. The primary neurons of the reflex arc include the vestibular nerve afferents (8<sup>th</sup> cranial nerve vestibulocochlear nerve), vestibular nuclei neurons, the extra ocular motor nuclei (3<sup>rd</sup>, 4<sup>th</sup>, and 6<sup>th</sup> cranial nerve) neurons which form the oculomotor nerves (Figure 1). For example, if you rotate your head to the left (counter clockwise), the endolymph in the lateral semicircular canals has a relative clockwise movement. This movement causes a displacement of the hair cell bundles towards the utricle (utriculopedal movement), exciting the hair cells in the left lateral canal. The synapses of the 8<sup>th</sup> nerve afferent excite the left or ipsilateral vestibular nuclei neurons involved in the VOR. The



axons of these neurons cross the midline and activate the right abducens motor neurons. The axons of the abducens motor neurons innervate the right lateral rectus muscle causing an abduction of the right eye. At the same time, the axons of the left vestibular VOR neurons excite internuclear neurons in the left abducens motor neurons. The axons of these internuclear neurons travel anteriorly in the medial longitudinal fasciculus to innervate the motor neurons in the medial rectus division of the 3<sup>rd</sup> or oculomotor nucleus. The axons of these motor neurons innervate the left medial rectus muscle to cause adduction of the left eye. Thus, there is a conjugate, or paired, almost instantaneous reflex movement of the eyes in the orbit causing them to counter rotate to the right. In addition, complementary neurons, located in the VOR pathway are disfacilitated resulting in the relaxation of the eye muscles in the opposing direction (right medial rectus and left lateral rectus). During a rotational stimulus to the left your eye approaches a rotational limit to the right. In this case, a saccade or fast eye movement brings the eye back to the midline.

A number of studies have measured the VOR in rodents (1, 4, 14, 17, 19, 24). Quinn et al. (1998a) tested the horizontal AVOR (angular VOR) during vertical axis rotations (upright yaw) in the dark: AVOR because only the canals are stimulated by this motion. Eye movements were recorded using an implanted scleral search coil. For stimulus frequencies of 0.05 to 2 Hz, they found the rat horizontal AVOR had a significant phase lead for frequencies below 0.1Hz. For frequencies above 0.5 Hz, the AVOR response was compensatory with a phase lead of approximately +1.1° and a gain of 0.5. The results of this study primarily reported the efficacy of the implanted coil

technique but also provided important baseline data on the frequency dependence of the horizontal AVOR during vertical axis rotations.

Later experiments examined how both information from canals and otolith organs converge as a whole during vertical and horizontal axis rotations. Brettler et al. (2000) studied the contributions of both semicircular canals and otolith organ input to the VOR by stimulating only the canals (vertical axis rotations) and both canals and otolith organs (horizontal axis rotations) in the rat (4). During vertical axis rotations (upright yaw), the horizontal AVOR response was present at both middle and high frequencies (0.2-2 Hz). The gains increased as the frequency increased and the phase response was compensatory at middle frequencies and higher (0.5 Hz and 1Hz). During horizontal axis rotations (nose-up yaw), the gain response remained fairly constant as the frequency increased but the phase values were compensatory across the whole range of frequencies tested. Overall, gain responses during horizontal and vertical axis rotations had almost the same values at middle frequencies of 0.5 Hz and the phase values were more compensatory during horizontal axis rotations compared to vertical axis stimulation which activates only the canals. This demonstrates that during horizontal axis rotations canal and otolith input are not independent of each other.

### ***III. Het Mice***

A spontaneous mutation, known as the *Head Tilt* or *het* mouse results is an animal that lacks otoconia (3, 22, 29). The function of the macula is affected only in the homozygous *het* mutant mice. However, the function of the semicircular canals and the cochlea (including middle ear structures) appears to be normal (14). Behavioral

manifestations of the homozygous *het* mutation include head tilt and inability to swim or float, but they are able to rotate under water (3, 23, 28). The *het* mouse model therefore provides a unique opportunity to study the contribution of otolith organs to vestibular function.

Next, a study by Jones et al. (1999) questioned whether the otolith organs in the *het* mouse were functional at all. They tested whether the *het* mouse could generate a vestibular evoked potential (VsEPs), recorded from the skull, in response to linear acceleration pulses. This study provided evidence that linear acceleration stimuli could not elicit VsEPs in the *het* mice. They concluded that the far-field vestibular responses to pulsed linear acceleration depended on intact otolith end organs (18). In other words, the stimuli adequate for eliciting linear vestibular evoked potentials VsEPs in normal mice do not evoke linear VsEPs in *het* mice. The otolith organs in *het* mice are not functional.

The function of both the otolith organs and the semicircular canals during vertical and horizontal axis rotations (AVOR) has also been studied in the mouse. In the recent study by Harrod & Baker (2003), the interaction between the semicircular canals and the otolith organs was examined in the *het* mouse and compared to normal wild type mice. Their results also support the idea that the semicircular canals and the otolith organs do not function independently. In order to test semicircular canal stimulation with and without otolith input, animals were subjected to five different stimulus movements: upright roll (horizontal rostro-caudal axis), on tail yaw (horizontal dorso-ventral axis), and inverted roll (horizontal rostro-caudal axis) for dynamic canal and otolith stimulus; upright yaw (vertical dorso-ventral axis) and on tail roll (vertical rostro-caudal axis) for

dynamic canal stimulation only. During horizontal axis rotations (sinusoidal upright roll, on tail/nose up yaw, and inverted roll), the AVOR response showed compensatory slow phase eye movements at frequencies of 0.05 Hz and 0.5 Hz for the control group but the *het* mice showed an out of phase response. The gain response increased as the frequency increased for both animals but the control group had higher gain values compared to the *het* mice. During vertical axis rotations (upright yaw, on tail roll), both groups had less VOR phase response at 0.05 Hz compared to 0.5 Hz. The VOR phase response was compensatory at the higher stimulus frequency of 0.5 Hz. The VOR response had low VOR gains at 0.05 Hz but had modest gains at 0.5 Hz for both animals, but control groups still showed higher gain values compared to *het* mice. Overall, VOR gain values during horizontal axis rotations were greater than the average gain elicited during vertical axis rotations. The VOR gain was nearly absent at 0.05 Hz in the absence of dynamic otolith stimulation during vertical axis rotation. Finally, the phase of the VOR response was compensatory during horizontal axis rotations at 0.05 Hz and 0.5 Hz compared to the vertical axis rotations.

#### ***IV. Purpose***

The purpose of this study is to test a fundamental question regarding the integration of vestibular signals in producing head movement-related oculomotor behaviors. The AVOR has been shown by Brettler et al. (2000) to be a contribution of both canals and otolith organs. In the *het* mouse, Harrod et al (2003) also found that the otolith organs contribute to AVOR at stimulus frequencies up to 0.5 Hz. The present study involved recording the horizontal AVOR in normal and *het* mice, and comparing the resultant

phase and gain response characteristics. Therefore, the present experiment expanded on the Harrod et al. (2003) study by increasing the stimulus frequency to 2 Hz ( $\pm 50^\circ/\text{sec}$ ) and the stimulus amplitude to  $\pm 100^\circ/\text{sec}$  (1Hz).

The influence of stimulus amplitude on both the phase and gain of the VOR shows a nonlinear response in the vestibular system of the mouse (1). Alphen et al. (2001) demonstrated that for all amplitudes the VOR response showed properties of a high-pass filter in that the gain increased and phase lead increased as frequency was increased. Harrod et al. (2003) found that the VOR response in the *het* mouse was significantly different compared to control groups at middle (0.5 Hz) and low (0.05 Hz) frequencies during  $\pm 50^\circ/\text{sec}$  amplitudes for stimulating only canals (upright yaw on tail roll) and both otolith organs and canals (vertical rotations). This in turn, suggests that VOR responses from the canals depended on the otolith organs for normal performance. Also, VOR gain during horizontal axis rotations was greater than the average gain elicited during vertical axis rotations. It could be hypothesized that the horizontal angular VOR (AVOR) in the *het* mouse has different response characteristics than that of normal mice, whose oculomotor reflexes are “calibrated” to input reflecting the coding of angular and linear accelerations by the semicircular canals and the maculae. It is proposed that the use of the *het* mouse is a method of examining the physiological systems affected by the genetic mutation as it relates to oculomotor behaviors. The strain of mice from which the mutant animals are derived served as the stock for the control studies. As an animal lacking otoconia, but without any other known phenotypic deficiencies resulting from the *het* mutation, the *het* mouse is an ideal model for studying selective labyrinthine sensory

deprivation to a loss of input from these specific receptors (14, 18). The mutation present in the *het* mouse allows for the isolation of changes and sensory losses similar to those found in microgravity environments.

## MATERIALS AND METHODS

All procedures followed the principles of laboratory animal care set forth by the National Institutes of Health Guide for Care and Use of Laboratory Animals and were approved by the Institutional Animal Care and Use Committee at NASA Ames Research Center and at San Jose State University (Protocol # 855). Animals were housed under the Animal Care Facility at NASA Ames Research Center and under the government guidelines. All procedures to implant the mouse head holder were followed as described in previous studies (17, 24).

### *I. Mice*

The normal C57BL/6 wild-type (*het/+*) and C57BL/6 *het* (*het/het*) mice, weighing approximately 10 grams, were obtained from the laboratory of the University of Missouri. Some *Het* animals exhibited a subtle head tilt compared to wild type, but otherwise maintained normal postures and locomotion. In order to identify otoconial deficiencies, the University of Missouri used swimming behaviors to identify the *het* phenotype. *Het* mice cannot swim, and when placed in a tank of water they cannot orient to the gravitational force vector and must be rescued (23, 29). The swim tests were performed at the University of Missouri and the mice were labeled as *het/het* mice (homozygous) and *het/+* mice-wild type (heterozygous) based on the results. In the present study, a total of 33 animals were used. Of those 33 animals, data was gathered on 12 animals (12 C57BL/6). Eight of the 12 C57BL/6 mice (4 *het* and 4 normal) provided the AVOR data reported here. All twelve animals were euthanized and tissue processed

for histology. The 21 animals remaining from the original 33 could not be successfully recorded. Some of these animals were euthanized due to post-surgical complications.

## ***II. Surgery***

To ensure proper restraint of the head during eye movement recordings, an acrylic pedestal was stereotaxically implanted onto the skull of each mouse using sterile procedures under anesthesia. Animals were anesthetized with an intraperitoneal administration (0.06 cubic centimeters, cc) of ketamine/xylazine cocktail. The effect of this initial dose lasted 60-90 minutes, after which supplemental intraperitoneal maintenance doses of the cocktail (0.03cc) were given if necessary. Body temperature was maintained throughout the surgical procedure by placing the mouse on a heating pad. Anesthesia was monitored through close observation of respiratory rate, limb tension, tail pinch, and corneal reflex. The animal was placed in the stereotaxic holder using blunt-tipped, non-traumatic ear bars to prevent labyrinth damage. A midline incision was made to expose the dorsal cranial surface, and the skull was scraped clean of tissue and muscle. Small screws were placed in the major cranial plates in order to anchor the implant to the skull (17, 24). During the implant procedure, the nose of the mouse was tilted downward at approximately 35° so that the horizontal semicircular canals were positioned in the horizontal plane during rotation and VOR recording (17, 24). Finally, dental acrylic was used to cover the head holder and the cranial screws. Care was taken to insure that edges around the head holder were smooth.



### ***III. Coil Fabrication and Calibration***

The eye movements were recorded and measured by using the scleral search coil method (4, 18). The coils were made using 0.008 inch diameter wire coiled to 100 turns and held together with cyanoacrylate (superglue). The average diameter of the entire coil was 0.6 mm. The resistance of the coils ranged from 18 – 35 ohms. This resulted in coils with sensitivities around 0.5 – 0.8V/° of eye movement (Figure 2). The mice were handled daily and allowed to adapt to the restraint and coil system prior to beginning the recording experiments. Before each recording session, the selected eye coil was calibrated prior to being placed in the eye. The calibration consisted of recording the response of the coil to a series of small horizontal and vertical rotational displacements (0°, ±5°, and ±10°). This calibration allowed us to calculate the coil's sensitivity. The mouse was secured to the recording platform by coupling the head post to the restraint mechanism (Figure 3). The right eye was anesthetized with ophthalmic tetracaine. Tetracaine was re-applied every 20-30 minutes as needed. The eye coil was then glued to the corneal surface directly over the pupil using medical grade cyanoacrylate glue. The glue was allowed to dry for several minutes. The horizontal eye coil signal was “zeroed” by rotating the animals' position within the field coils, after which the whole apparatus was placed within the Specimen Test Container (STC) aboard the Multi-Axis Centrifuge (Vestibular Research Facility, NASA/Ames).

#### ***IV. Equipment***

The Multi-axis Centrifuge (Figure 4) within the Vestibular Research Facility (VRF) is designed to measure the physiological responses to angular or combined linear and angular accelerations in small animals. The centrifuge is constructed with symmetrical outer yolk assemblies fixed to the main body. Each assembly is equipped with an STC. In the current configuration, only one arm of the centrifuge has been upgraded to meet system performance specifications. There are 4 axes of motion: a main spin axis, an outer high performance spin axis, an inner high performance spin axis, and an inner positioning axis. In this experiment, we only utilized the main spin axis and the outer high performance spin axis. The body of the centrifuge rotates about the main spin axis at a maximum rate of  $240^\circ/\text{s}$ . The STC is attached to the inner gimbal. The inner and outer gimbals are driven by high performance motors capable of achieving maximum peak velocities of  $\pm 500^\circ/\text{s}$ . Gimbal motors applied DC to 5 Hz angular motions (up to  $500^\circ/\text{sec}$  velocity and  $500^\circ/\text{sec}^2$  acceleration) to the STC and its payload. Also, fifteen electrically isolated slip-ring assemblies allowed the recording of multiple channels of electrophysiological data continuously during operation.

#### ***V. Stimulus Paradigms***

The VOR was measured from recordings of the animal's eye position and the velocity feedback signal driving the stimulus. The data, extracted from longer records, include head velocity ( $V_h$ , in degrees/sec) and eye position ( $P_e$ , in degrees). In this experiment, we used three different stimulus paradigms similar to Harrod & Baker (2003) study. First, horizontal axis rotations at constant velocities of  $\pm 50$  and  $\pm 100^\circ/\text{s}$  were

applied four times for  $\pm 50^\circ/\text{s}$  at the beginning of the session and two times for  $100^\circ/\text{s}$  at the end of the session. Second, sinusoidal oscillations followed after the runs of  $\pm 50^\circ/\text{s}$ . For  $\pm 50^\circ/\text{s}$  and  $\pm 100^\circ/\text{s}$ , sinusoidal rotations were measured at frequencies of 0.05, 0.10, 0.25, 0.50, 1.00, and 2.00 Hz ( $\pm 50^\circ/\text{s}$  only) for two different amplitudes of peak velocity. In order to hold peak velocity constant across the range of stimulus frequencies, the rotation amplitude was varied. Finally, centrifugation was combined with horizontal rotations of  $\pm 90^\circ/\text{s}$ . Animals were used once a week for each run and/or sessions.

## ***VI. Data Analysis***

The data was recorded and extracted using custom software developed in LabVIEW. The stored eye position records were then low-pass filtered and differentiated using the Wave Metrics (IGOR Pro 5) software package. Using IGOR, the calculations of gain were first determined from detecting all the maximum and minimum values (positive or negative) of the eye velocity. This program allowed us to use the curve fitting function, fitting a sine wave to the eye velocity. The fitted curve allowed us to detect the low frequency amplitudes located in these peaks and to average them for each cycle. After calculating all the peaks we obtained the absolute value of those amplitudes and then these values were used to calculate the mean and the standard deviation for both eye velocity and stimulus. The amplitude mean of the peaks of eye velocity divided by the amplitude of the stimulus was the gain value. In order to calculate the phase values in IGOR, the temporal difference between the stimulus and eye velocities was calculated. The phase values were reported as phase errors for the proximity values of the ideal VOR compensation. The phase lead was calculated by adding  $180^\circ$  from all the mean values of

each run. Phase lead indicated the values for comparing the ideal VOR compensation. If the VOR phase lead was close to 0° (opposite direction of both the eye velocity and stimulus), VOR compensation was present. In addition, a VOR phase of 180° was the anticomensatory VOR response of both eye velocity and stimulus moving in the same direction. All the average values of gain and phase were entered into a spread sheet to calculate the mean of all the runs. These values were utilized for further statistical analysis and graphing bode diagrams showing both gains (ratio) and phase leads (°) values versus the frequency (Hz).

Statistical analyses were done using a nonparametric (Mann-Whitney) unpaired test with a two-tailed p-value ( $p < 0.05$ ) to compare both *het* mice and control groups for all the runs. For the present analysis, *het* mice (n=4) and normal mice (n=4) were used, each animal underwent at least two test sessions on different dates.

## ***VII. Histology***

Mice were euthanized with carbon dioxide and promptly decapitated. Inner ears were extracted, dissected, and washed three times in neutral phosphate buffered saline (PBS), pH 7.4, followed by constant agitation for twenty minutes. The washes continued with distilled water, repeating the three cycles followed by constant agitation for twenty minutes. Using a capsule knife and microprobes, the maculae of the saccule and utricle, and otoconial membranes, if present, were dissected at room temperature.

### ***VIII. Scanning electron microscopy (SEM)***

For SEM examination, samples were attached to a carbon conductive tab (12mm) and placed on an aluminum specimen mount (1/2" Slotted head, 1/8" Pin). Samples were then dried at room temperature and coated with a thin layer of gold using a PELCO SC-7 sputter coater. Coated samples were examined in a LEO 1450 VP scanning electron microscope (BioVISCenter Electron Microscopy facility).

## RESULTS

### *I. Microscopy of the Otoconial Mass in the Het Mouse*

The morphology of the otoconial mass, including the otoconial membrane and the otoconia, was determined by microdissection, light microscopy and scanning electron microscopy (SEM). The inner ears were harvested from each mouse (n=8) and the condition of the otoconial mass was noted in each case. During microdissection of the *het* mouse inner ear, it was observed that the utricle and saccule had a significant reduction in the number of otoconia. The saccule was preserved for SEM while the utricle was lost during dissection. During SEM observation of one *het* mouse, the remaining saccular otoconia were less regular in shape than the wild type and some few were larger (Figure 5). The microdissection confirmed the normal morphological structure of the utricle, saccule, and semicircular canals, cochlea, oval window, and bones of the middle ear (stapes, incus, and malleus) for every mutant.

### *II. Vestibulo-ocular Reflex*

#### *A. General features of Vertical axis horizontal VOR (upright yaw)*

Example recordings from one normal mouse are shown for both amplitudes of peak velocity, 50°/s (Figures 6, 7, 8, 9, 10, 11) and 100°/s (Figures 12, 13, 14, 15, 16). In figures 6 through 27, eye position (°) is shown at top of the graph. Eye position records show slow eye movements interrupted by fast saccades. This value is differentiated into eye velocity (°/s) in the middle of the graph. Finally, the stimulus or head velocity (°/s) is shown at the bottom of the graph. Eye velocity during the slow phase of the VOR was compared to head velocity to compute gain (Figures 28 and 29). At low frequencies (less

than 0.1Hz) and a velocity of 50°/s, the VOR response to the stimulus is weak (Figures 6 and 7). At higher frequencies (0.25Hz and greater) and a velocity of 50°/s, the slow and fast phases of the VOR response becomes more apparent. The data shows the VOR response increased as stimulus frequency (Hz) was increased. At the higher stimulus velocity of 100°/s, slow phase eye movement was present at low frequencies (Figure 12). Compensatory eye movements were readily apparent at 0.25Hz and greater (Figures 14, 15, 16). At higher stimulus frequencies, the amplitude of the eye movement is decreased and therefore saccades are not present (Figures 14 and 16). In contrast, the VOR responses of the *het* mouse were more attenuated for both 50°/s (Figures 17, 18, 19, 20, 21, and 22) and 100°/s (Figures 23, 24, 25, 26, and 27). In Figures 25, 26, 27, the VOR response is present at frequencies of 0.25Hz and greater but more attenuated during stimulus amplitude of 50°/s.

#### *B. Frequency dynamics of control group and het mice compared*

Gain is defined as the ratio of the eye velocity to head velocity. Phase is the temporal difference between the stimulus velocity and the eye velocity expressed in degrees. Therefore, a gain of 1.0 and a phase difference of 0° would represent perfect compensation. The average gain in the response of four animals was calculated for each frequency. The VOR response showed frequency dependence for both *het* mice (n=4) and control groups (n=4). Using a nonparametric (Mann-Whitney) unpaired test with a two-tailed p-value ( $p < 0.05$ ) indicated the significant values for all the frequencies in both *het* mice and control groups. Figure 28, is a Bode plot for the 50°/s data comparing the *het* mice with the control mice. The VOR gain in the control mice was greater for all

frequencies tested but only significant at 0.25 (gain;  $0.42 \pm 0.069$ , p-values  $< 0.05$ ) and 0.50Hz (gain;  $0.46 \pm 0.068$ , p-values  $< 0.05$ ) during  $50^\circ/\text{s}$ . For the  $100^\circ/\text{s}$  stimulus, the gain values for the control mice were significantly greater across all frequencies (Figure 29) showing p-values less than 0.05.



## DISCUSSION

The results of this study indicated that the gain of the horizontal angular vestibulo-ocular reflex (AVOR) in *het* mice (n=4) and the control group (n=4) increased as the intensity of the stimulus increased. In both cases the AVOR attempts to match (or compensate for) the stimulus. Previous studies in the *het* mouse using sections stained for light microscopy and fluorescence microscope images suggested the complete absence of otoconia in the utricle and saccule (23, 28). In this study, SEM images of one *het* mouse saccule revealed a greatly decreased number of otoconia and those remaining otoconia were abnormally shaped. This condition could account for the decrease in the gain observed in this study. In turn, the function of the central neurons receiving input from both canal and otolith organs would also be affected. The result is a reduction in the strength of the oculomotor reflex (Figure 30).

Moving the animal in such a way that the canals are stimulated and otolith organs are not (upright yaw), resulted in gain and phase changes as the frequency stimulus increased (4, 14). Harrod & Baker (2003) also observed that the VOR response in normal and *het* mice was highly attenuated with large phase errors at 0.05 Hz and a more modest VOR phase errors at 0.5 Hz. The VOR gain was absent at 0.05Hz (gain of 0.05 in normal group and gain of 0.001 in *het* mice) due to the absence of stimulation to the otolith system during vertical axis rotations. VOR responses were shown during middle frequency rotation of 0.5Hz with gain values of 0.24 in normal mice and 0.11 in *het* mice. Brettler et al (2000) also found VOR response in normal rats was minimal for stimulus frequencies under 0.2Hz by stimulating the canals in the upright yaw and nose-up roll

position. During upright yaw position, the phase errors of the reflex were small from 0.5 to 2 Hz (2° at 0.5 Hz, 3° at 1 Hz, 0° at 2 Hz) and the gain was fairly constant near 100%. In our study, the VOR gain at low frequencies of 0.05Hz was also low as predicted from previous studies. There was a dependency of frequencies (0.05Hz-2Hz) resulting in an increase of VOR gain values from 0.2 to 0.4 in *het* mice and from 0.3 to 0.5 in normal mice.

This study is consistent with previous research (4, 14) emphasizing that the receptors from both canals and otolith are necessary inputs to the central neurons in order to achieve a normal AVOR. Inputs from both receptor types contribute to the output of the VOR response. Also, the results suggest that the abnormal VOR output of the *het* mouse could be due to a change in the input to the vestibular nuclei neurons that receive convergence input. These neurons may continue to receive activity from the otolith afferent nerve but it could be reduced. One might have assumed that both the *het* and normal mice would have the same AVOR since morphologically the canals are normal in the *het* mouse. Based on the results of this study, there are differences of AVOR between the *het* and normal groups. A study by Bush et al (1993) showed spatiotemporal convergence of canal and otolith input onto the vestibular nuclei neurons in rats using a combination of linear and angular acceleration stimuli. The results showed that the vestibular nuclei neurons exhibited a complex spatiotemporal response. If it is assumed that the *het* mouse has a comparable population of convergent vestibular nuclei neurons, then this could explain the abnormal AVOR in the *het* mouse. Further research is necessary to examine how the mechanisms underlying the change in the AVOR have

occurred. These experiments would include stimulating both canals and otoliths (4, 14) 2000) applying different rotational stimuli (e.g., horizontal rostro-caudal axis in upright roll, horizontal rostro-caudal axis in inverted roll) and various VOR adaptation paradigms.

The convergence of both canals and otolith has been shown in a few other species by using electrical stimuli and examining different combinations of head rotations. One such study (Zhang X., et al 2002) showed that 30 to 40% of cells recorded in the vestibular nuclei in cats received convergent inputs from both anterior semicircular canal (AC) and utricular (UT) nerves. The outputs of these central neurons are still unknown. Recording from the afferent nerves in *het* mice could provide a better explanation of the convergence of canals and otolith organs onto the central neurons during angular head acceleration.

In addition, there are several studies that have shown the function of both canals and otoliths in different species by characterizing the output of primary afferents. For example, Goldberg and Fernandez (1971) showed that during passive whole-body rotation in head-restrained animals, vestibular afferents originating in the semicircular canals of the squirrel monkey encode the angular velocity of the head-in-space. Another study (Scudder and Fuchs 1992) showed that the vestibular afferents of rhesus monkeys project to second-order neurons within the vestibular nuclei, which encode angular head velocity during the compensatory eye movements generated by VOR. However, the vestibular nuclei also receive projections from many structures that could influence their discharge. For example, neck muscle spindle afferents are known to influence the

activity of vestibular nuclei neurons in decerebrate animals (Boyle and Pompeiano 1981). Another study (Sato et al. 2002) suggested that during mixed angular head accelerations, the vestibulocollic reflex (VCR) could be accomplished by the vestibulospinal (VS) and vestibulo-oculospinal (VOS) convergent neurons. This study showed that 18% of the vestibular nucleus neurons in cats received convergent inputs from the nerves of the anterior semicircular canals (AC) and posterior semicircular canals (PC). 82% of these AC/PC activated vestibulospinal (VS) and vestibulo-oculospinal (VOS) reflexes. During stimulation of the horizontal semicircular canal (HC) and/or PC nerves, 24% of vestibular nucleus neurons received convergent inputs from both nerves and 46% of these HC/PC activated VS and VOS reflexes. Therefore, the convergence of multiple inputs to the vestibular nuclei is an important feature of how these signals are processed and used to control common reflex motions.

Understanding the contribution of the canals and otolith organs to horizontal AVOR is still not clear. Studying the structure and function of the vestibular endorgans and their neural connections is providing information concerning their contribution to AVOR. Because the brain has the ability to process information in different ways, this enables it to respond to a changing environment. One area of interest has been or would be to study the motor pathways of the cerebellum (personal communication; Dr. Richard Boyle and Dr. Geoffrey Bush from Vestibular Research Facility at NASA Ames Research Center). The use of a different animal model such as the knock-out/in mouse (e.g., NR2c subunit receptor in the granular layer of the cerebellum) may help us

understand how the nervous system responds to microgravity and serves to improve the health of patients with neurological problems that cause impairment of balance (2, 11).

## BIBLIOGRAPHY

1. Alphen AM, Stahl JS, Zeeuw CI. "The dynamic characteristics of the mouse horizontal vestibule-ocular and optokinetic response." Brain Research 890 (2001): 296-305.
2. Bacal K, Billica R, Bishop S. "Neurovestibular symptoms following space flight." Journal of Vestibular Research 13 (2003): 93-102.
3. Bergstrom B, You Y, Erway LC, Lyon MF, Schimenti JC. "Deletion mapping of the head tilt (*het*) gene in mice: a vestibular mutation causing specific absence of otoliths." Genetics 150 (1998): 815-822.
4. Brettler S, Rude SA, Quinn KJ. "The effect of gravity on the horizontal and vertical vestibulo-ocular reflex in the rat." Experimental Brain Research 132 (2000): 434-444.
5. Boyle R, Pompeiano O. "Responses of vestibulospinal neurons to sinusoidal rotation of the neck." Journal of Neurophysiology 44 (1981): 633-649.
6. Bush G, Perachio AA, Angelaki AD. "Encoding of head acceleration in vestibular neurons. 1. Spatiotemporal response properties to linear acceleration." Journal of Neurophysiology 6 (1993): 2039-2055.
7. Clarke AH, Schonfeld U, Helling K. "Unilateral examination of utricle and saccule function." Journal of Vestibular Research 13 (2003): 215-225.
8. Collewijn H. Adaptive Mechanism in Gaze Control, Facts and Theories. New York: Academic Press, 1985: 51-69.
9. Fernandez C, Lysakowski A, Goldberg JM. "Hair cell counts and afferent innervation patterns in the cristae ampullares of the squirrel monkey with a comparison to the chinchilla." Journal of Neurophysiology 73 (1995): 1253-1269.
10. FitzGerald MJT, Folan-Curran J. Clinical Neuroanatomy and Related Neuroscience. New York: W.B. Saunders, 2002: 163-168.
11. Furman JM, Hsu LC, Whitney SL, Redfern MS. "Otolith-ocular responses in patients with surgically confirmed unilateral peripheral vestibular loss." Journal of Vestibular Research 13 (2003): 143-151.
12. Golberg JM, Fernandez C. "Physiology of peripheral neurons innervating semicircular canals of the squirrel monkey. I. Resting discharge and response to constant angular accelerations." Journal of Neurophysiology 34 (1971): 635-660.

13. Goldberg JM, Lykakowski A, Fernandez C. "Morphological and ultrastructural studies in the mammalian cristae ampullares." Hearing Research 49 (1990): 89-102.
14. Harrod CG, Baker JF. "The vestibulo ocular reflex (VOR) in otoconia deficient head tilt (*Het*) mutant mice versus wild type C57BL/6 mice." Brain Research 972 (2003): 75-83.
15. Horch K, Dhillon G. "Vestibular Physiology." Neuroprosthetics 2 (2004): 1117.
16. Iurato S. Submicroscopic Structures of the Inner Ear. New York: Pergamon Press, 1967: 210-216.
17. Iwashita M, Kanai R, Funabiki K, Matsuda K, Hirano T. "Dynamic properties, interactions and adaptive modifications of vestibulo-ocular reflex and optokinetic response in mice." Neuroscience Research 39 (2001): 299-311.
18. Jones SM, Erway LC, Bergstrom RA, Schimenti JC, Jones TA. "Vestibular responses to linear acceleration are absent in otoconia-deficient C57BL/6J*Et-het* mice." Hearing Research 135 (1999): 56-60.
19. Katoh A, Kitazawa H, Itohara S, Nagao S. "Dynamic characteristics and adaptability of mouse vestibulo-ocular and optokinetic response eye movements and the role of the flocculo-olivary system revealed by chemical lesions." Proceedings of the National Academy of Sciences 95 (1998): 7705-7710.
20. Lewis ER, Leverenz EL, Bialek WS. The Vertebrate Inner Ear. Florida: CRC Press, 1985: 47-56.
21. Lim, D. J. Fine Morphology of the Otoconial Membrane and Its Relationship to the Sensory Epithelium. Columbus, OH: Ohio State University College of Medicine, 1979: 929-938.
22. Ornitz DM, Bohne BA, Thalmann I, Harding GW, Thalmann R. "Otoconial agenesis in tilted mutant mice." Hearing Research 122 (1998): 60-70.
23. Paffenholz R, Bergstrom RA, Pasutto F, Wabnitz P, Munroe RJ, Jagla W, Heinzmann U, Marquardt A, Bareiss A, Laufs J, Russ A, Stumm G, Schimenti JC, Bergstrom DE. "Vestibular defects in head-tilt mice result from mutations in *Nox3*, encoding an NADPH oxidase." Research Communication 18 (2004): 486-491.
24. Quinn KJ, Rude SA, Bettler SC, Baker JF. "Chronic recording of the vestibulo-ocular reflex in the restrained rat using a permanently implanted scleral search coil." Journal of Neuroscience Methods 80 (1998a): 201-208.

25. Sato H, Imagawa M, Meng H, Zhang X, Bai R, Uchino Y. "Convergence of ipsilateral semicircular canal inputs onto single vestibular nucleus neurons in cats." Experimental Brain Research 145 (2002): 351-364.
26. Scudder C.A, Fuchs F. "Physiological and behavioral identification of vestibular nucleus neurons mediating the horizontal vestibuloocular reflex in trained rhesus monkeys." Journal of Neurophysiology 68 (1992): 244-264.
27. Squire LR, Bloom FE, McConnell SK, Roberts JL, Spitzer NC, Zigmond MJ. Fundamental Neuroscience. Orlando, FL: Academic Press, 2003: 873-893.
28. Sweet, H. Head tilt (*het*). Mouse Newsletter 63 (1980): 19.
29. Xue B, Skala K, Jones T, Hay M. "Diminished baroreflex control of heart rate responses in otoconia-deficient C57BL/6J*Ei* head tilt mice." American Journal Physiology Heart Circulatory Physiology 287 (2004): H741-H747.
30. Zhang X, Sasaki M, Sato H, Meng H, Bai R.S, Imagawa M, Uchino Y. "Convergence of the anterior semicircular canal and otolith afferents on cat single vestibular neurons." Experimental Brain Research 147 (2002): 407-417.



## **APPENDIX: FIGURES**

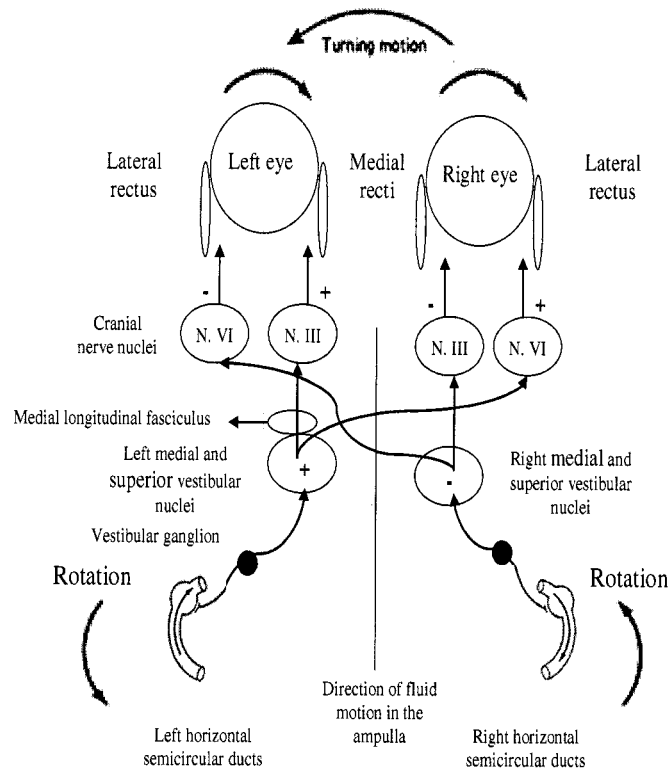


Figure 1. Vestibulo-ocular Reflex (VOR) Bio-circuit showing the primary neural pathway of the reflex arc.



Figure 2. *Scleral Search Coil*. Coil was glued to the cornea over the pupil of the right eye. Copper wire coil (0.008 inch diameter, 100 turns, 1.0 mg approx.) held together with superglue

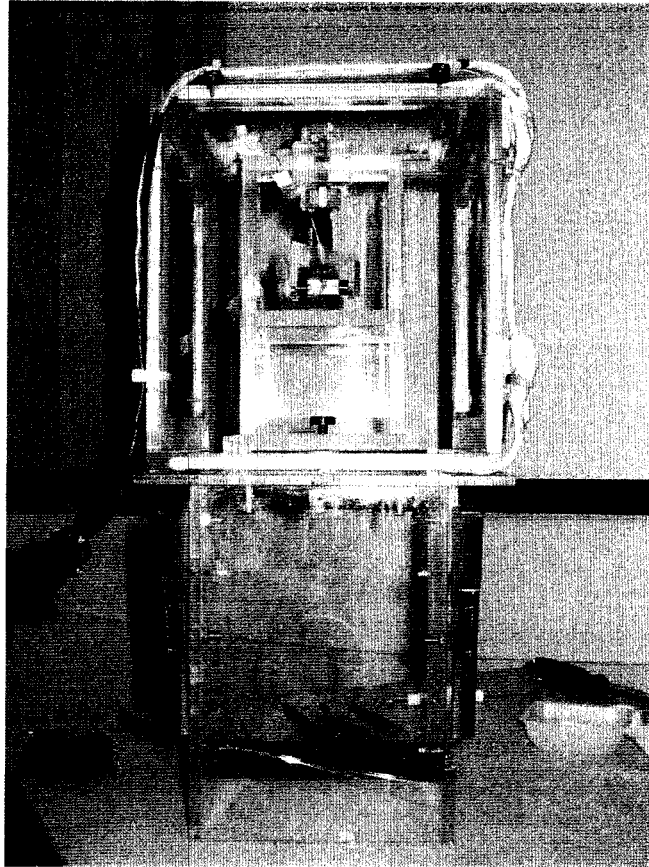


Figure 3. *Animal restraint apparatus mounted within a field coil system for recording the murine AVOR.* The restraint mechanism allowed the animal's position within the field coil (outer cubicle frame) to be adjusted fore-and-aft as well as vertically. The platform of this restraint apparatus facilitated the rotations for angular recordings of the coil calibration. The center post was the structure to which the head-implanted pedestal was attached, while the body rested on top of the platform. This apparatus was labeled as the "specimen test container" of the Multi-Axis Centrifuge at NASA/Ames' Vestibular Research Facility

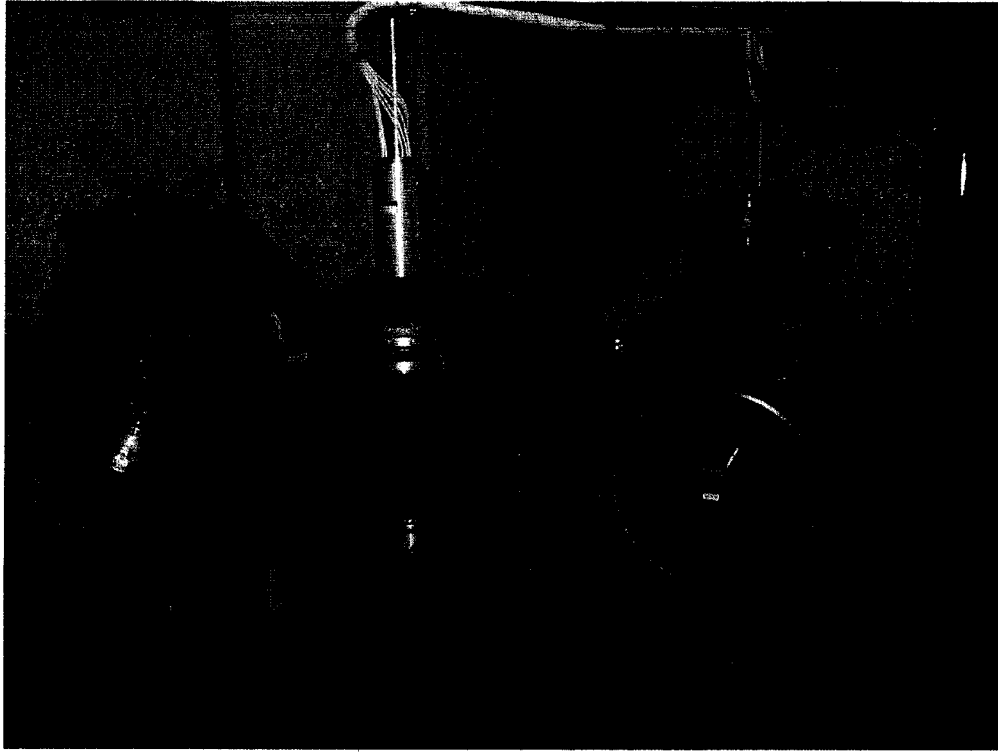


Figure 4. *Multi-axis Centrifuge; Vestibular Research Facility.* The four axes of rotation; a main spin axis, an inner and outer high performance axes, and an inner positioning axis, when used in combination allowed complex motions delivering both angular and linear accelerations

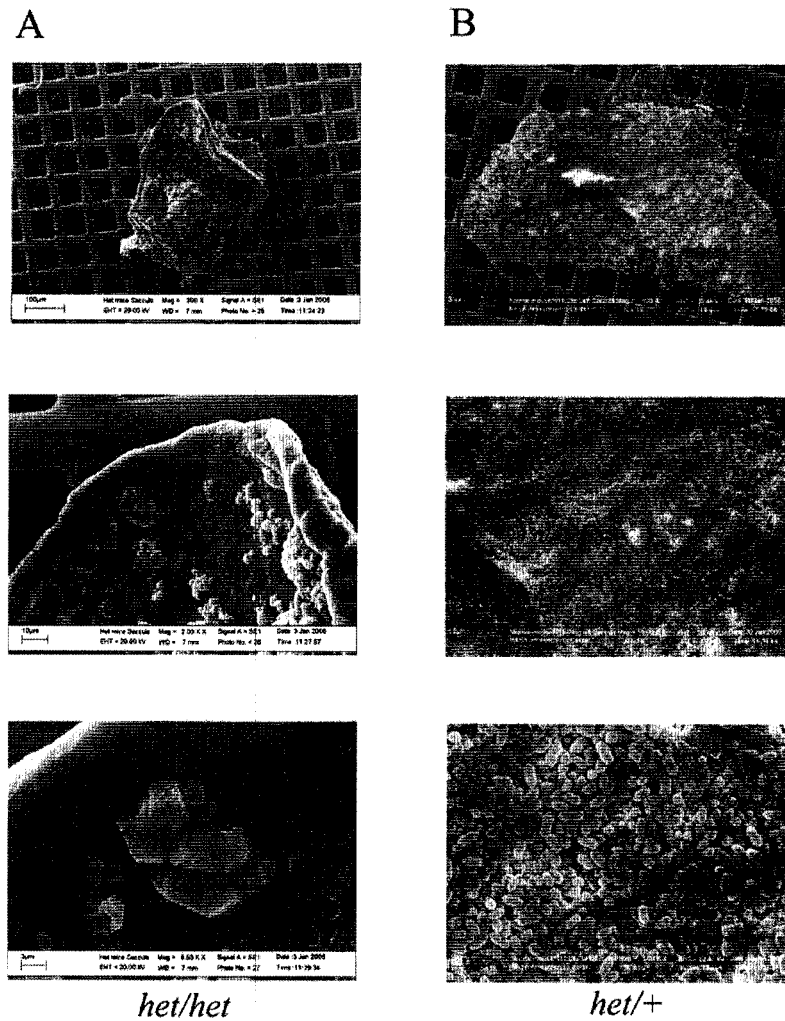


Figure 5. Scanning electron microscopy (SEM) showing the abnormal structures of the otoconia formation of the head tilt mutant (*het/het*) at different magnifications. (A) At low magnification (300X), parts of the saccule (left side) are shown and some indications of abnormal density of otoconia. Middle (2.0 KX) and higher (6.5 KX) magnifications showed the morphological structure of the otoconia detecting the deterioration of the composition. (B) Normal phenotype animal (*het/+*) showing parts of the saccule (left side) and normal otoconia formation and density at different magnifications compared to *het/het* mutation

## Control group (50°/sec)

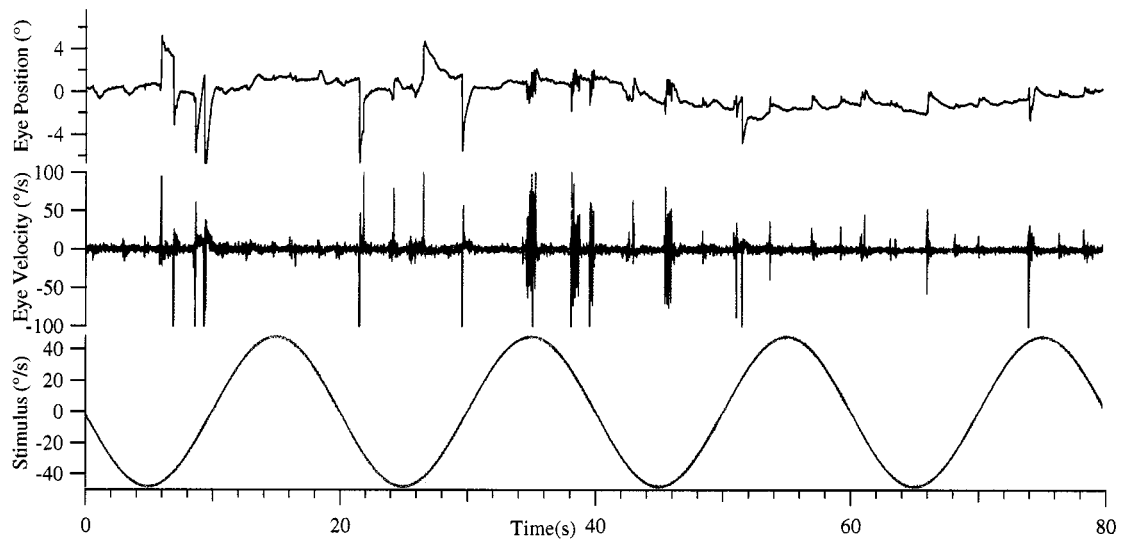


Figure 6. Horizontal eye movement traces of normal mice at frequency of 0.05Hz during vertical axis rotations, up-right yaw in the dark. The first trace (*black*) shows the eye position in degrees, the second trace (*blue*) represents the eye velocity in degrees per second, and the third trace (*red*) indicates the stimulus velocity in degrees per second. VOR gain was 0.294 and phase was  $-3.8^\circ$

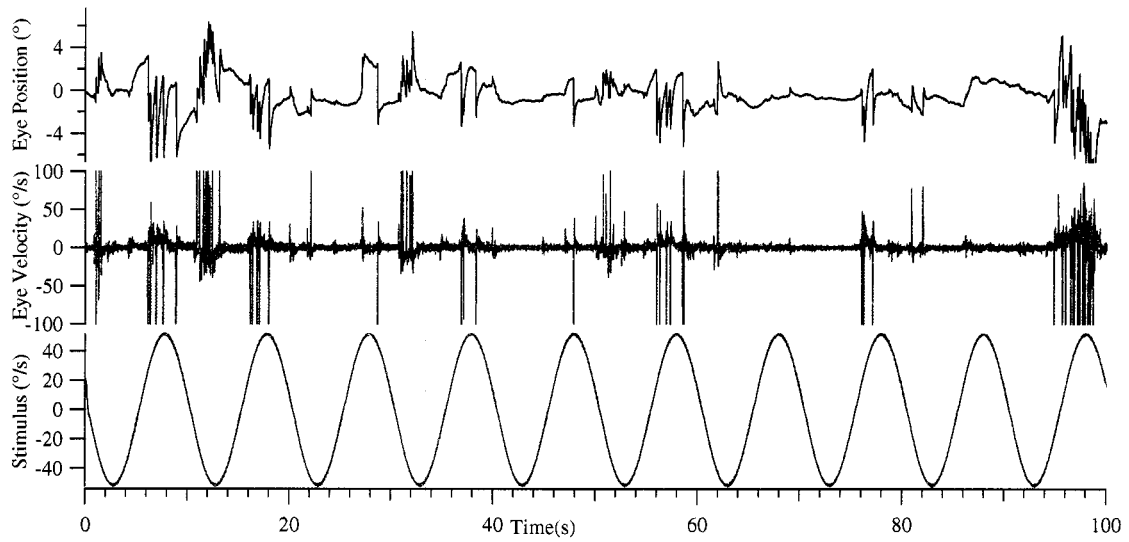


Figure 7. Horizontal eye movement traces of normal mice at frequency of 0.1Hz during vertical axis rotations, up-right yaw in the dark. The first trace (*black*) shows the eye position in degrees, the second trace (*blue*) represents the eye velocity in degrees per second, and the third trace (*red*) indicates the stimulus velocity in degrees per second. VOR gain was 0.308 and phase was  $-36.9^\circ$

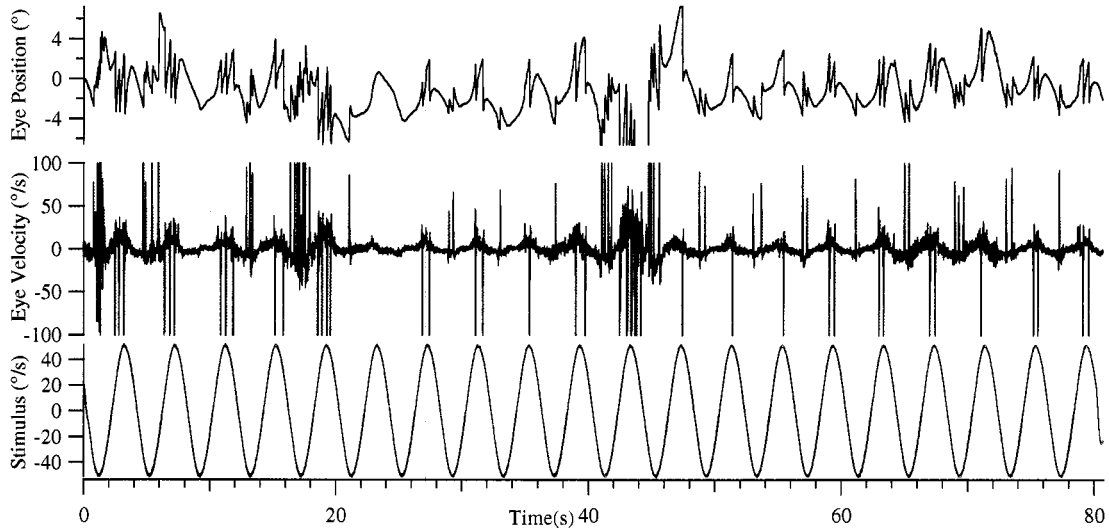


Figure 8. Horizontal eye movement traces of normal mice at frequency of 0.25Hz during vertical axis rotations, up-right yaw in the dark. The first trace (*black*) shows the eye position in degrees, the second trace (*blue*) represents the eye velocity in degrees per second, and the third trace (*red*) indicates the stimulus velocity in degrees per second. VOR gain was 0.489 and phase was  $29.4^\circ$



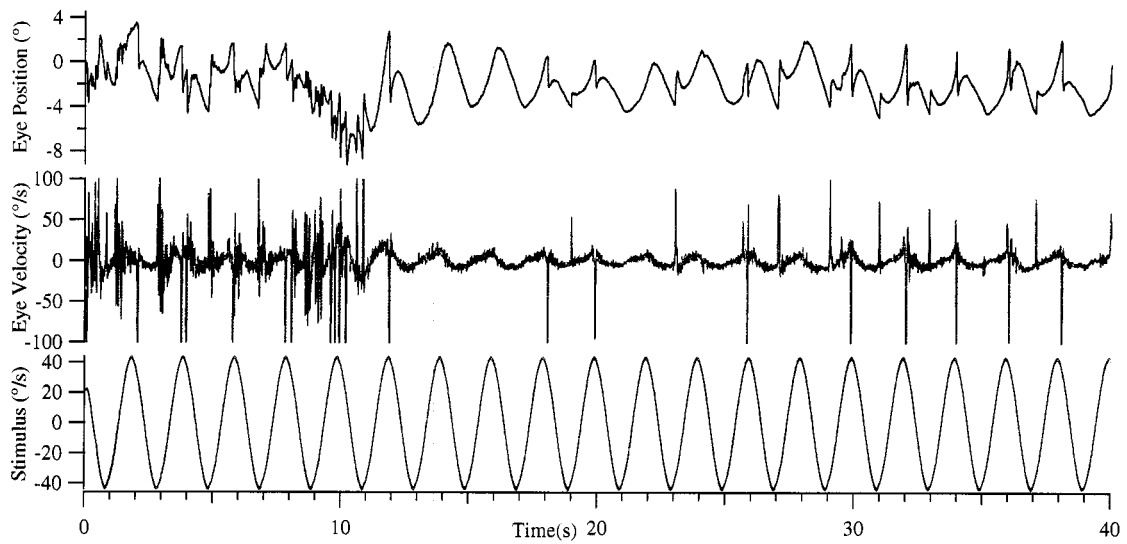


Figure 9. Horizontal eye movement traces of normal mice at frequency of 0.5Hz during vertical axis rotations, up-right yaw in the dark. The first trace (*black*) shows the eye position in degrees, the second trace (*blue*) represents the eye velocity in degrees per second, and the third trace (*red*) indicates the stimulus velocity in degrees per second. VOR gain was 0.441 and phase was  $157.5^\circ$

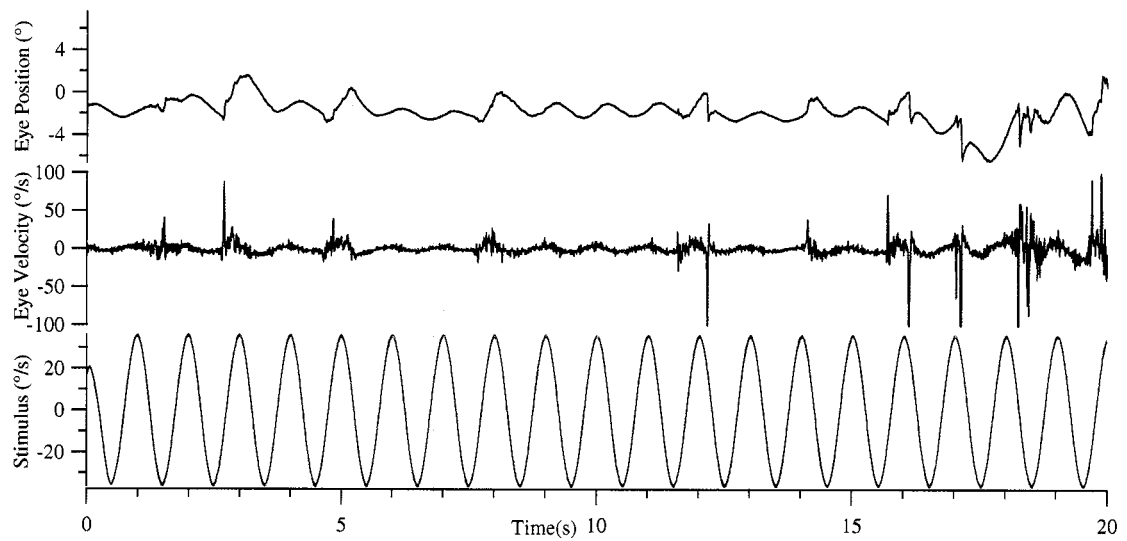


Figure 10. Horizontal eye movement traces of normal mice at frequency of 1Hz during vertical axis rotations, up-right yaw in the dark. The first trace (*black*) shows the eye position in degrees, the second trace (*blue*) represents the eye velocity in degrees per second, and the third trace (*red*) indicates the stimulus velocity in degrees per second. VOR gain was 0.357 and phase was  $128.2^\circ$

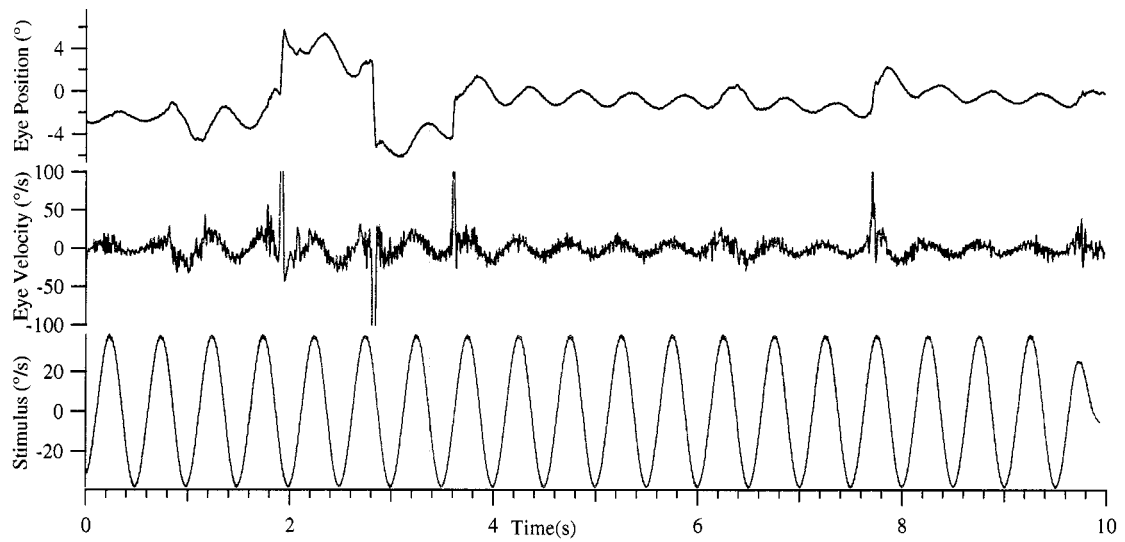


Figure 11. Horizontal eye movement traces of normal mice at frequency of 2Hz during vertical axis rotations, up-right yaw in the dark. The first trace (*black*) shows the eye position in degrees, the second trace (*blue*) represents the eye velocity in degrees per second, and the third trace (*red*) indicates the stimulus velocity in degrees per second. VOR gain was 0.683 and phase was 102.1°

## Control group (100°/sec)

---

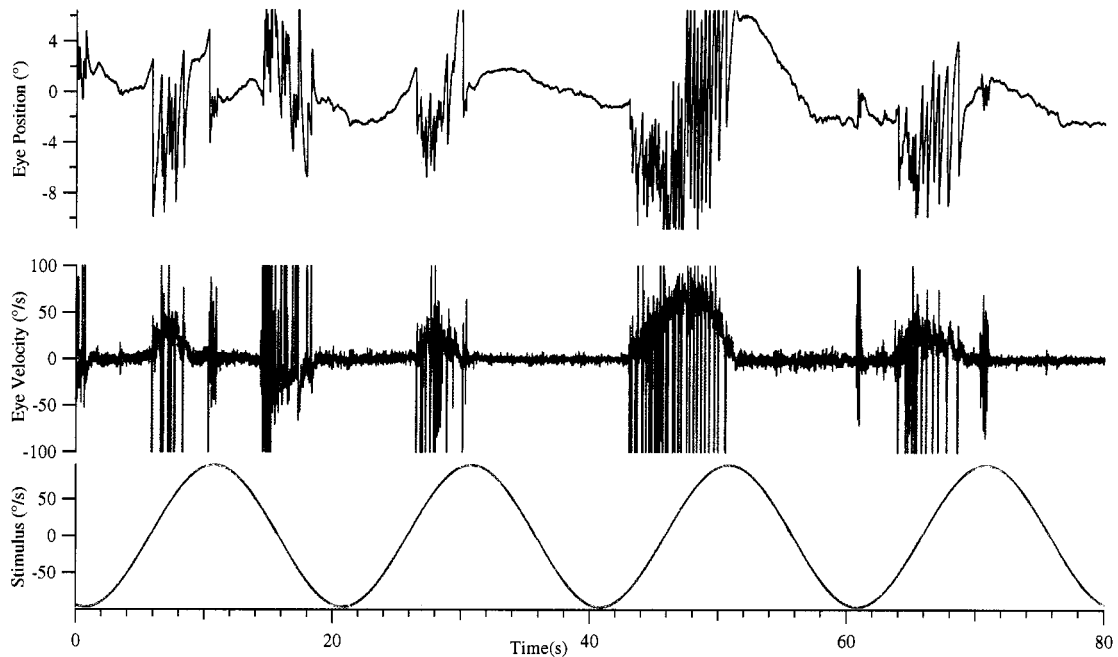


Figure 12. Horizontal eye movement traces of normal mice at frequency of 0.05Hz during vertical axis rotations, up-right yaw in the dark. The first trace (*black*) shows the eye position in degrees, the second trace (*blue*) represents the eye velocity in degrees per second, and the third trace (*red*) indicates the stimulus velocity in degrees per second. VOR gain was 0.442 and phase was 5.3°

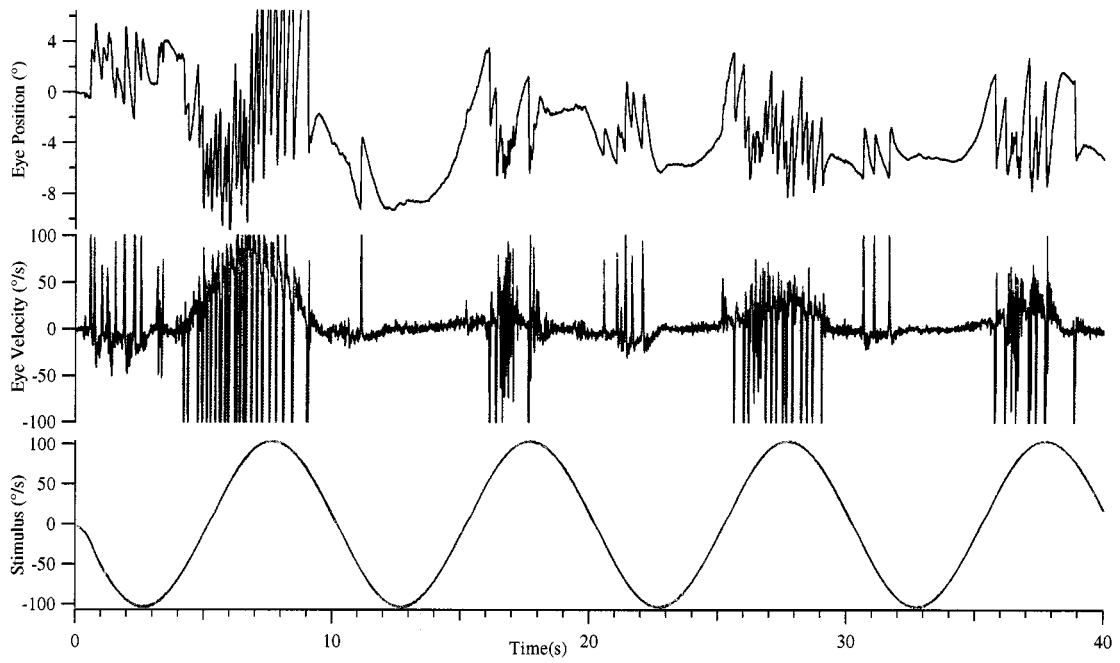


Figure 13. Horizontal eye movement traces of normal mice at frequency of 0.1Hz during vertical axis rotations, up-right yaw in the dark. The first trace (*black*) shows the eye position in degrees, the second trace (*blue*) represents the eye velocity in degrees per second, and the third trace (*red*) indicates the stimulus velocity in degrees per second. VOR gain was 0.399 and phase was 108.3°

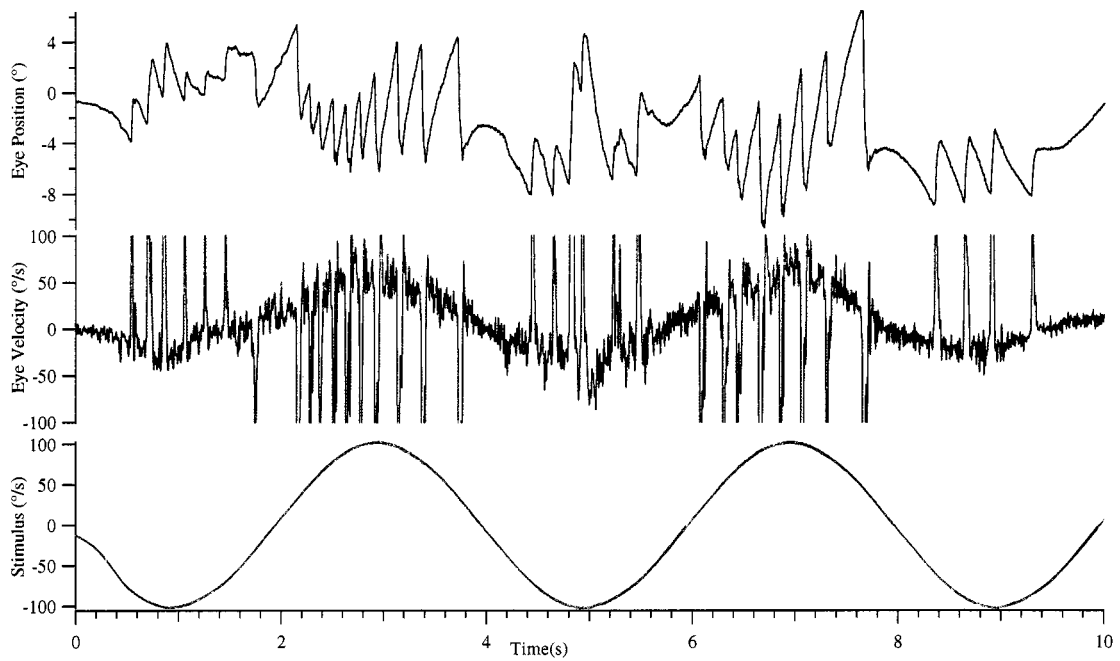


Figure 14. Horizontal eye movement traces of normal mice at frequency of 0.25Hz during vertical axis rotations, up-right yaw in the dark. The first trace (*black*) shows the eye position in degrees, the second trace (*blue*) represents the eye velocity in degrees per second, and the third trace (*red*) indicates the stimulus velocity in degrees per second. VOR gain was 0.488 and phase was  $32.8^\circ$

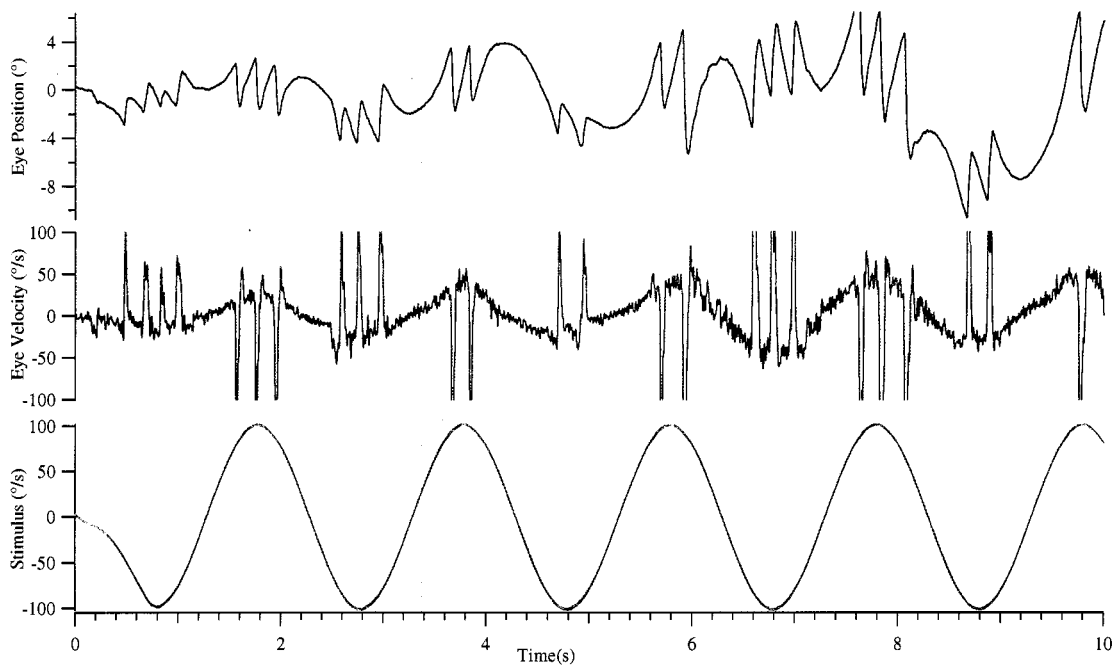


Figure 15. Horizontal eye movement traces of normal mice at frequency of 0.5Hz during vertical axis rotations, up-right yaw in the dark. The first trace (*black*) shows the eye position in degrees, the second trace (*blue*) represents the eye velocity in degrees per second, and the third trace (*red*) indicates the stimulus velocity in degrees per second. VOR gain was 0.416 and phase was 55.1°

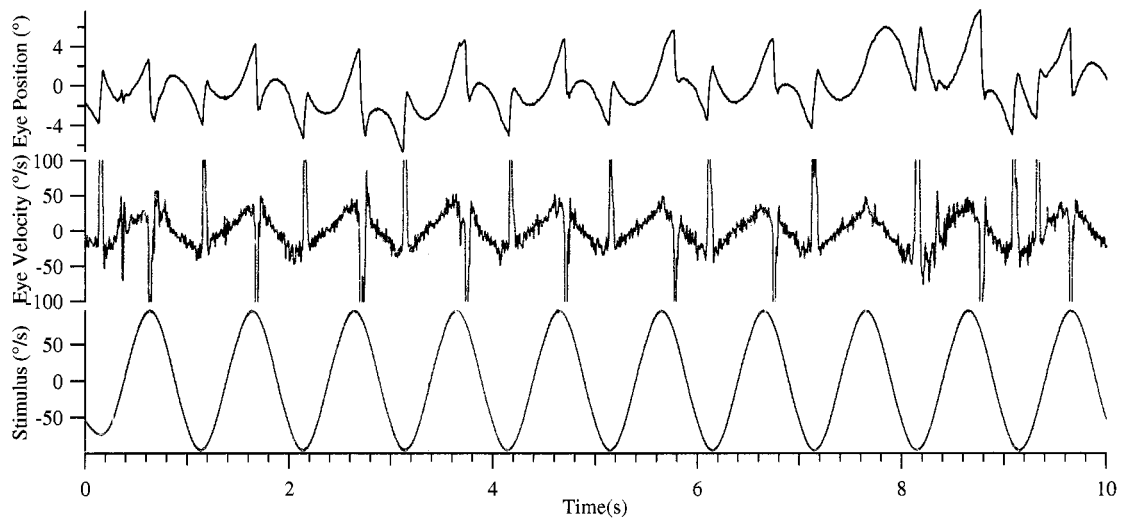


Figure 16. Horizontal eye movement traces of normal mice at frequency of 1Hz during vertical axis rotations, up-right yaw in the dark. The first trace (*black*) shows the eye position in degrees, the second trace (*blue*) represents the eye velocity in degrees per second, and the third trace (*red*) indicates the stimulus velocity in degrees per second. VOR gain was 0.411 and phase was  $69.1^\circ$

## Het mice (50°/s)

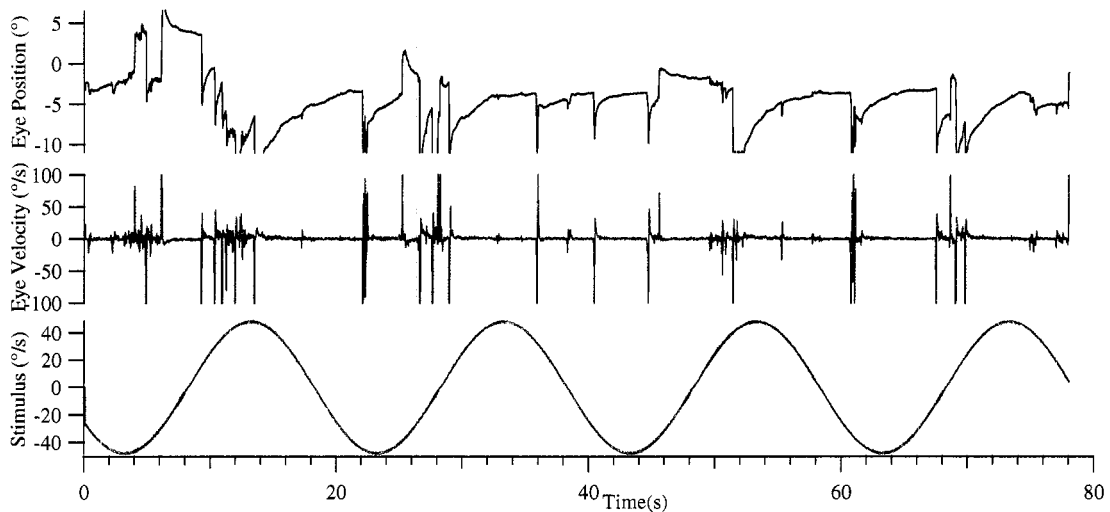


Figure 17. Horizontal eye movement traces of *het* mice at frequency of 0.05Hz during vertical axis rotations, up-right yaw in the dark. The first trace (*black*) shows the eye position in degrees, the second trace (*blue*) represents the eye velocity in degrees per second, and the third trace (*red*) indicates the stimulus velocity in degrees per second. VOR gain was 0.349 and phase was  $31.3^\circ$

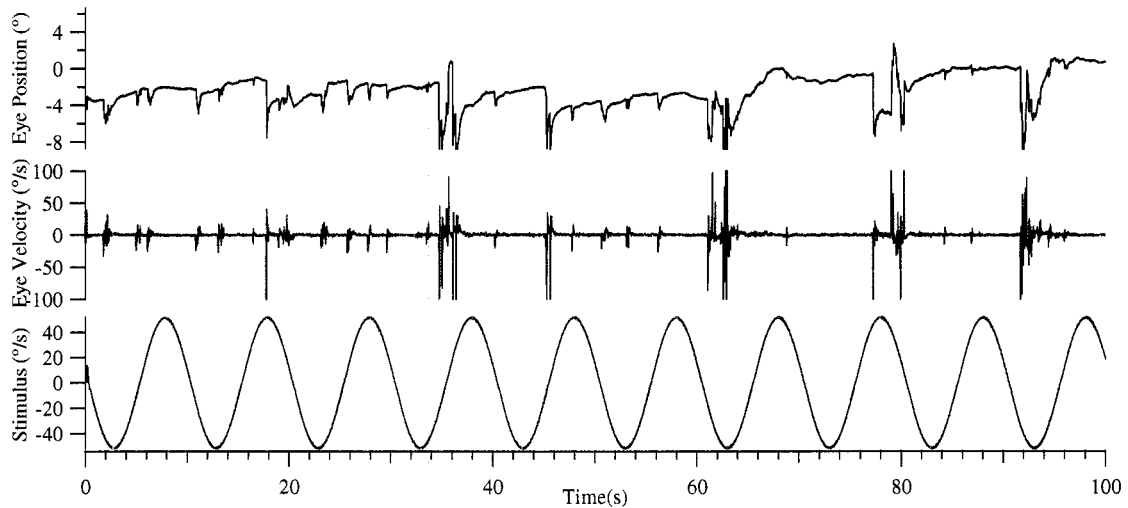


Figure 18. Horizontal eye movement traces of *het* mice at frequency of 0.1Hz during vertical axis rotations, up-right yaw in the dark. The first trace (*black*) shows the eye position in degrees, the second trace (*blue*) represents the eye velocity in degrees per second, and the third trace (*red*) indicates the stimulus velocity in degrees per second. VOR gain was 0.222 and phase was  $-69.6^\circ$



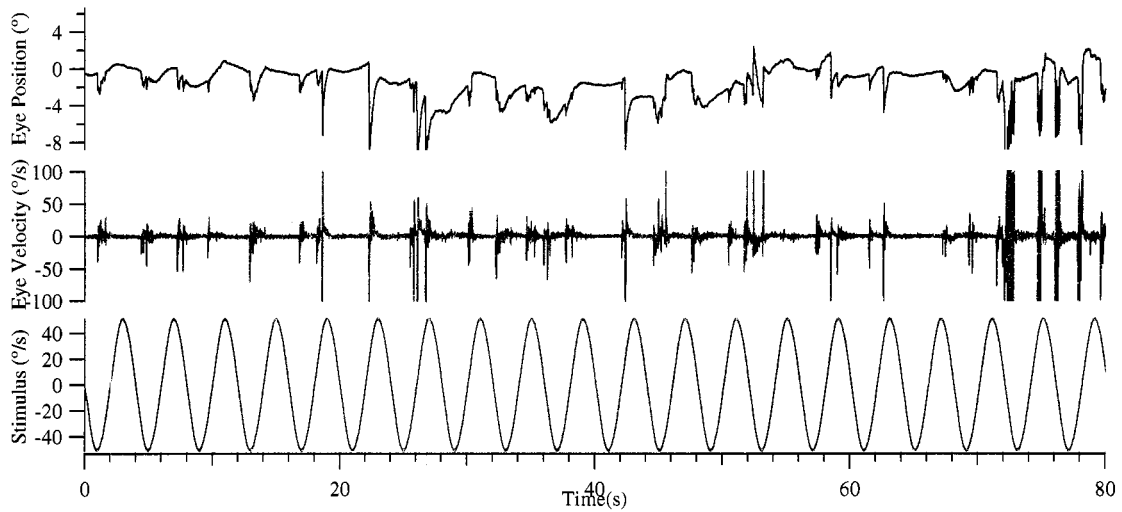


Figure 19. Horizontal eye movement traces of *het* mice at frequency of 0.25Hz during vertical axis rotations, up-right yaw in the dark. The first trace (*black*) shows the eye position in degrees, the second trace (*blue*) represents the eye velocity in degrees per second, and the third trace (*red*) indicates the stimulus velocity in degrees per second. VOR gain was 0.231 and phase was  $19.2^\circ$

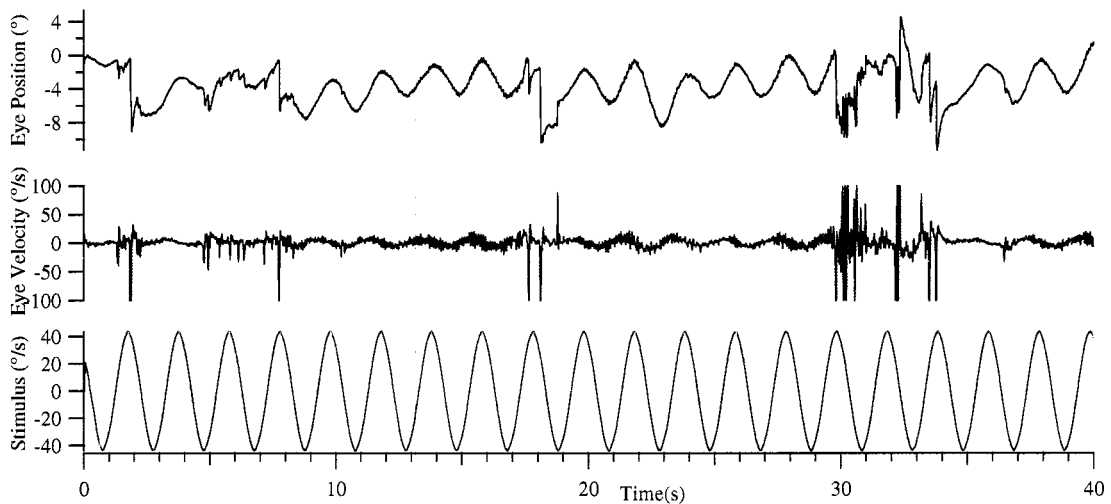


Figure 20. Horizontal eye movement traces of *het* mice at frequency of 0.5Hz during vertical axis rotations, up-right yaw in the dark. The first trace (*black*) shows the eye position in degrees, the second trace (*blue*) represents the eye velocity in degrees per second, and the third trace (*red*) indicates the stimulus velocity in degrees per second. VOR gain was 0.472 and phase was  $182.0^\circ$

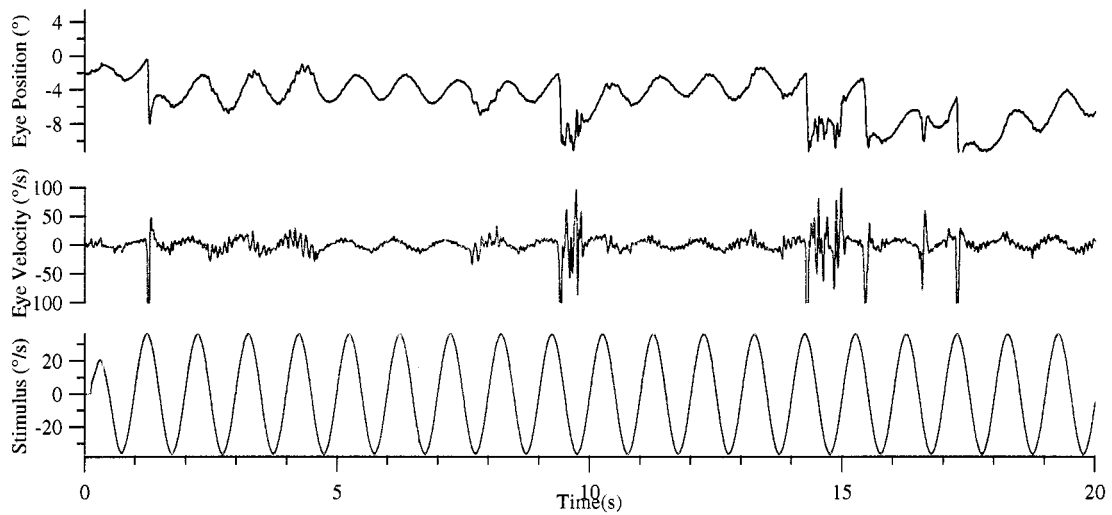


Figure 21. Horizontal eye movement traces of *het* mice at frequency of 1Hz during vertical axis rotations, up-right yaw in the dark. The first trace (*black*) shows the eye position in degrees, the second trace (*blue*) represents the eye velocity in degrees per second, and the third trace (*red*) indicates the stimulus velocity in degrees per second. VOR gain was 0.553 and phase was 173.6°

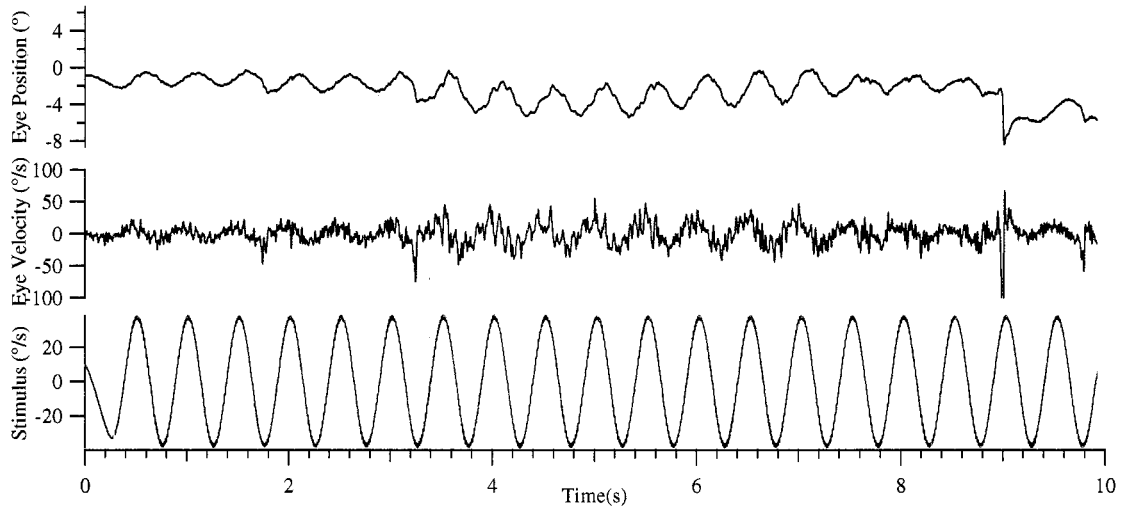


Figure 22. Horizontal eye movement traces of *het* mice at frequency of 2Hz during vertical axis rotations, up-right yaw in the dark. The first trace (*black*) shows the eye position in degrees, the second trace (*blue*) represents the eye velocity in degrees per second, and the third trace (*red*) indicates the stimulus velocity in degrees per second. VOR gain was 0.477 and phase was 40.6°

**Het mice (100°/sec)**

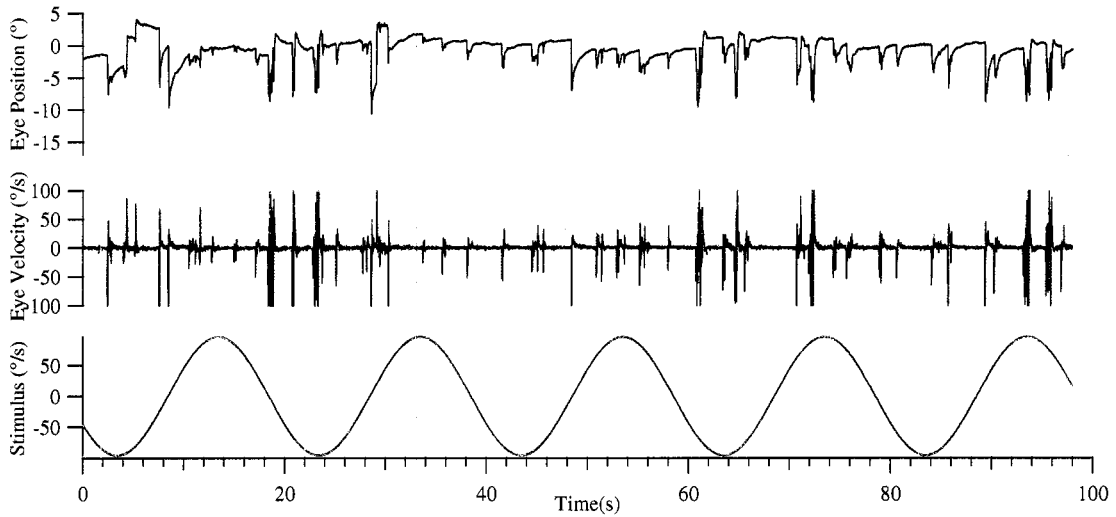


Figure 23. Horizontal eye movement traces of *het* mice at frequency of 0.05Hz during vertical axis rotations, up-right yaw in the dark. The first trace (*black*) shows the eye position in degrees, the second trace (*blue*) represents the eye velocity in degrees per second, and the third trace (*red*) indicates the stimulus velocity in degrees per second. VOR gain was 0.183 and phase was 177.5°

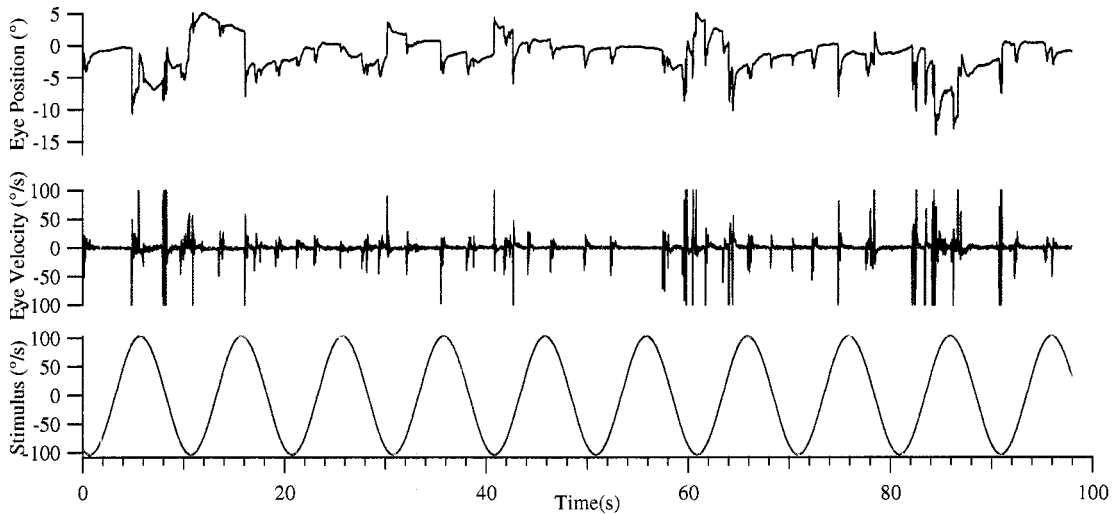


Figure 24. Horizontal eye movement traces of *het* mice at frequency of 0.1Hz during vertical axis rotations, up-right yaw in the dark. The first trace (*black*) shows the eye position in degrees, the second trace (*blue*) represents the eye velocity in degrees per second, and the third trace (*red*) indicates the stimulus velocity in degrees per second. VOR gain was 0.147 and phase was 44.7°

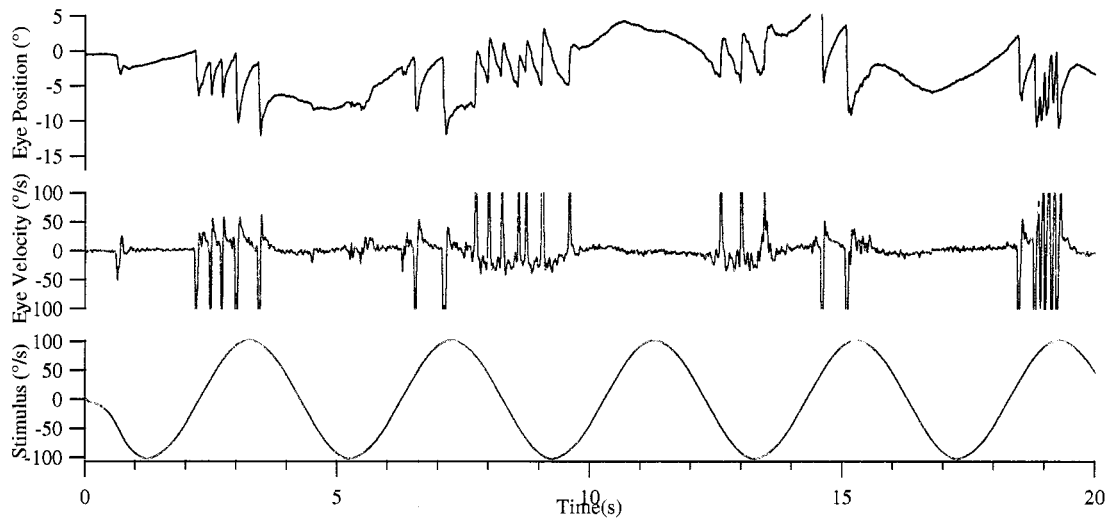


Figure 25. Horizontal eye movement traces of *het* mice at frequency of 0.25Hz during vertical axis rotations, up-right yaw in the dark. The first trace (*black*) shows the eye position in degrees, the second trace (*blue*) represents the eye velocity in degrees per second, and the third trace (*red*) indicates the stimulus velocity in degrees per second. VOR gain was 0.173 and phase was  $3.7^\circ$

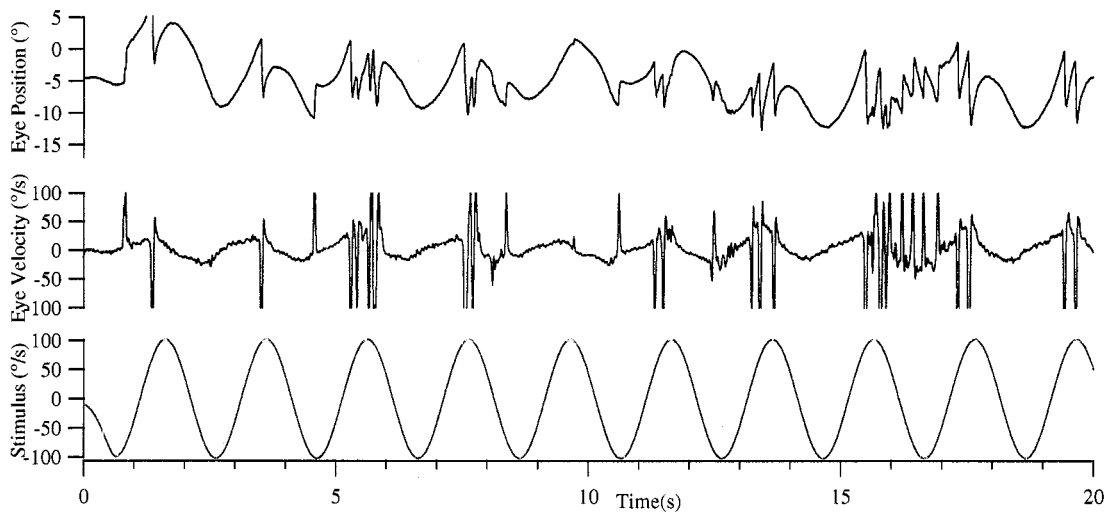


Figure 26. Horizontal eye movement traces of *het* mice at frequency of 0.5Hz during vertical axis rotations, up-right yaw in the dark. The first trace (*black*) shows the eye position in degrees, the second trace (*blue*) represents the eye velocity in degrees per second, and the third trace (*red*) indicates the stimulus velocity in degrees per second. VOR gain was 0.284 and phase was  $92.3^\circ$

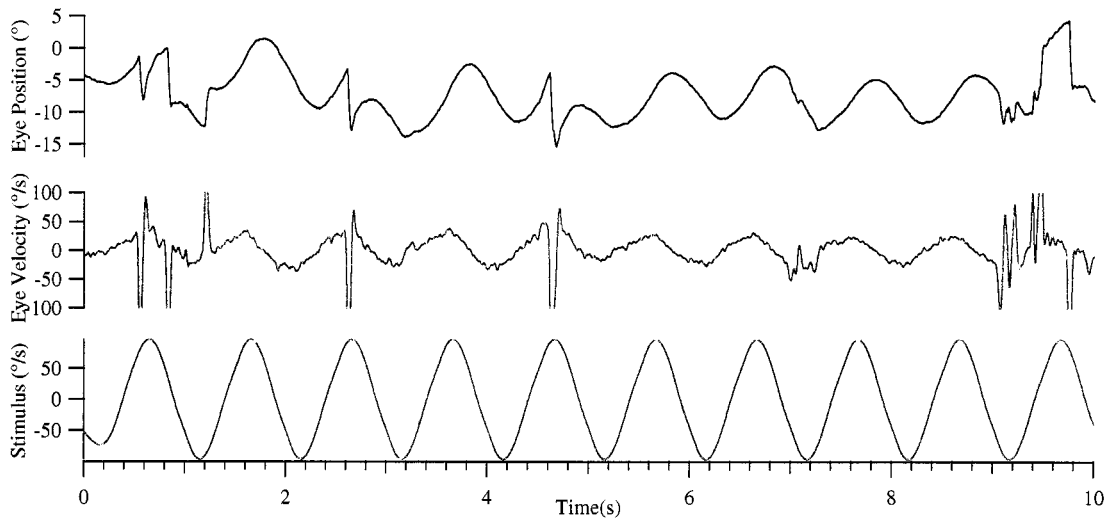


Figure 27. Horizontal eye movement traces of *het* mice at frequency of 1Hz during vertical axis rotations, up-right yaw in the dark. The first trace (*black*) shows the eye position in degrees, the second trace (*blue*) represents the eye velocity in degrees per second, and the third trace (*red*) indicates the stimulus velocity in degrees per second. VOR gain was 0.339 and phase was 181.4°

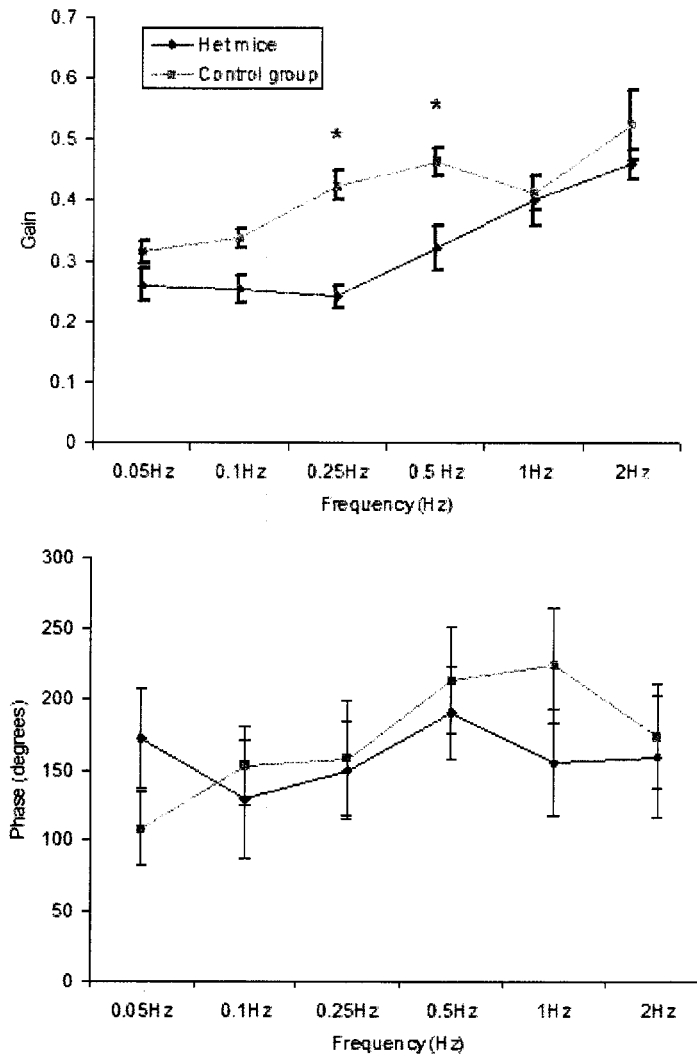


Figure 28. Bode diagrams ( $50^\circ/s$ ) of horizontal vestibulo-ocular reflex (VOR) in the *het* mice (blue) and control groups (pink) during upright yaw. Averaged gains (*upper panel*) are expressed as ratios of the value for upright yaw at each frequency (0.05Hz, 0.1Hz, 0.25Hz, 0.5Hz, 1Hz, and 2Hz) and phases (*lower panel*) are shown in degrees at each frequency. The two asterisks (\*) represent significant p-values less than 0.05 of gain values at frequencies of 0.25Hz and 0.5Hz

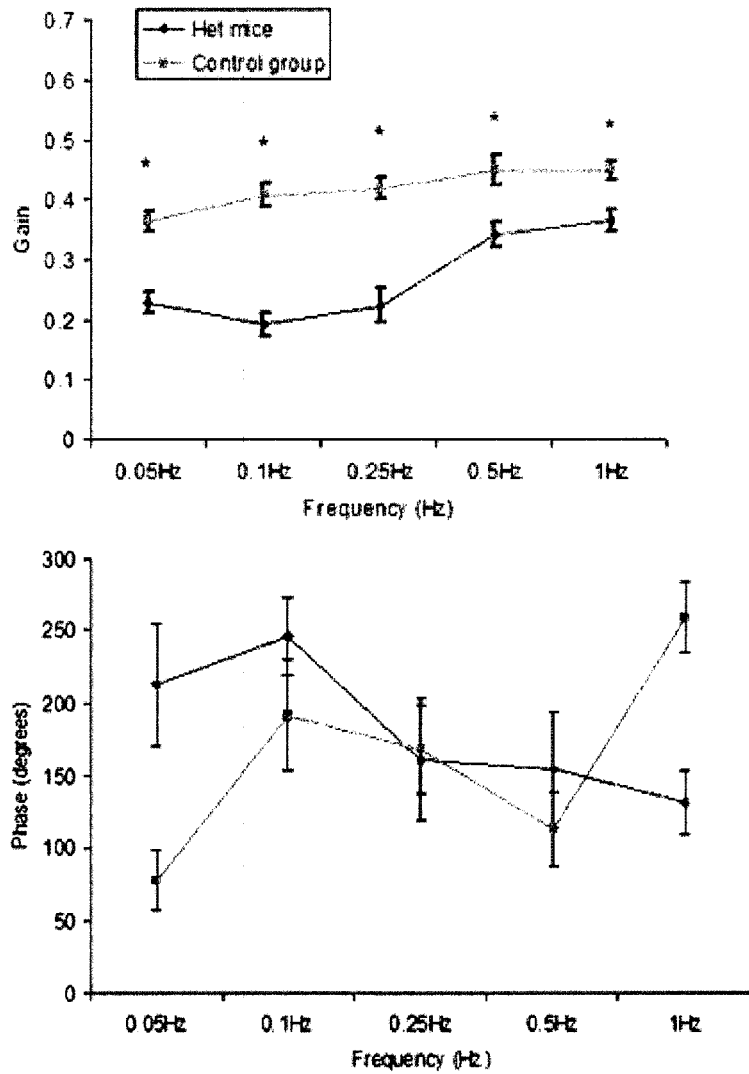


Figure 29. Bode diagrams ( $100^\circ/\text{s}$ ) of horizontal vestibulo-ocular reflex (VOR) in the *het* mice (pink) and control groups (blue) during upright yaw. Averaged gains (*upper panel*) are expressed as ratios of the value for upright yaw at each frequency (0.05Hz, 0.1Hz, 0.25Hz, 0.5Hz, 1Hz, and 2Hz) and phases (*lower panel*) are shown in degrees at each frequency. The two asterisks (\*) represent significant p-values less than 0.05 of gain values at all frequencies

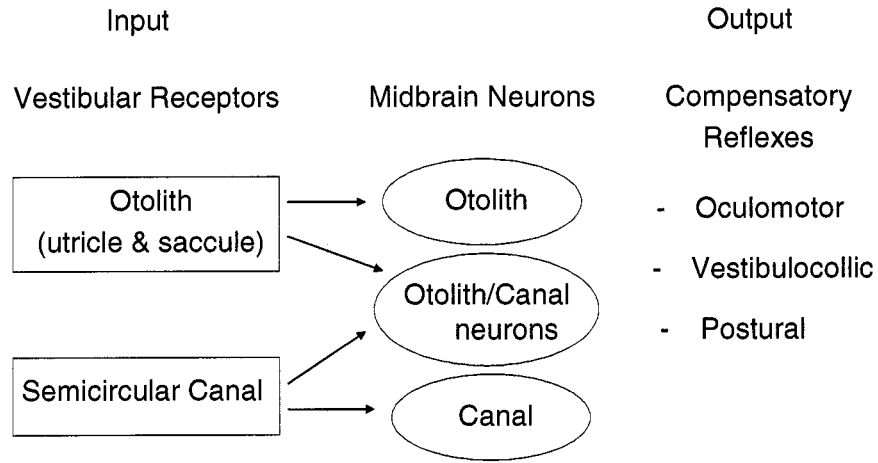


Figure 30. Function of the vestibular system as a whole showing three main components: the vestibular receptors (input), midbrain neurons, and the compensatory reflexes (output). *Het* mice show an abnormal output oculomotor reflex response (eye movement response) compared to the control groups (9, 12).